UNIVERSIDADE D
COIMBRA

Pedro Manuel Cardoso Amado

DYNAMIC SIMULATION AND OPTIMIZATION OF A CARNOT BATTERY USING HEAT PUMP/ORGANIC RANKINE CYCLES

Dissertação no âmbito do Mestrado em Engenharia Mecânica, ramo de Energia e Ambiente, orientada pelo Professor Doutor Ricardo António Lopes Mendes e Professor Doutor Márcio Duarte Albino dos Santos e apresentada ao Departamento de Engenharia Mecânica da Faculdade de Ciências e Tecnologia

Julho de 2022

FACULDADE DE CIÊNCIAS E TECNOLOGIA
UNIVERSIDADE D COIMBRA

Dynamic Simulation and Optimization of a Carnot Battery using Heat Pump/Organic Rankine Cycles

A dissertation submitted in partial fulfilment of the requirements for the degree of Master in Mechanical Engineering in the speciality of Energy and Environment

Simulação Dinâmica e Otimização de uma Bateria de Carnot utilizando Bombas de Calor e Ciclos de Rankine Orgânicos

Author

Pedro Manuel Cardoso Amado

Advisor[s]

Ricardo António Lopes Mendes

Márcio Duarte Albino dos Santos

Committee

Chair	**Professor Doutor José Manuel Baranda Moreira da Silva Ribeiro** **Assistant Professor – University of Coimbra**
Member	**Professor Doutor João Pedro da Silva Pereira** **Invited Assistant Professor – University of Coimbra**
Advisor	**Professor Doutor Márcio Duarte Albino dos Santos** **Invited Assistant Professor – University of Coimbra**

Coimbra, July, 2022

“The production of heat alone is not sufficient to give birth to the impelling power: it is necessary that there should also be cold; without it, the heat would be useless.”

Sadi Carnot, Réflexions sur la puissance motrice du feu et sur les machines propres à développer cette puissance, 1824

ACKNOWLEDGEMENTS

The present work, as well as the efforts leading up to its writing, were only possible thanks to all those who supported and motivated me throughout this journey.

I thank the professors who accompanied me and my colleagues through these 5 years, and who dedicated their efforts to empower and inspire their students. I would like to especially thank professor Ricardo Mendes, professor Márcio Santos, and professor José Baranda Ribeiro for all the time they dedicated in support of this dissertation, for their ideas and wisdom, and for continuously motivating me to do better and produce high quality work.

I thank those in my family who supported me through good and bad times, whose presence brought joy when it was most needed, and whose guidance kept me between the lines.

And finally, I give thanks to the friends who accompanied me during these difficult years – when all seemed lost, your companionship kept me grounded.

Abstract

With the efforts to decarbonize the energy sector comes a growing demand of electricity, most of which is to be supplied by renewable generation in a carbon-neutral future. To balance the variability inherent to most renewable energy sources, some form of energy storage is required.

In this work, a short review of current systems is made with a particular focus on Carnot Batteries, whose operating characteristics, long life and low environmental footprint make them competitive for daily energy storage. A transient model was developed to simulate the full operation of a Carnot Battery composed of Vapour Compression Heat Pump and Organic Rankine Cycles in conjunction with a sensible thermal storage, key performance parameters were identified, and a Pareto optimization was carried out by balancing costs and performance across 25 configurations of storage temperature spread and heat exchanger pinch point.

It was concluded that the wider storage spreads and higher pinch points lead to lower costs as they decrease the size of the water tank and the heat exchangers, and also to lower efficiencies as unfavourable temperature gradients are created for the heat pump and heat engine.

A Pareto front was identified, consisting of 10 configurations that were able to either optimize one criterion, or balance of two or more criteria, and conclusions were drawn as to the applicability of each configuration.

Keywords: Electric Energy Storage, Carnot Battery, Pumped Thermal Energy Storage, Vapour Compression Heat Pump, Organic Rankine Cycle

Resumo

Com a descarbonização do setor energético, será previsível um crescimento no consumo de energia elétrica, a maioria da qual será fornecida por fontes de geração renováveis. Para equilibrar esta variabilidade, será necessário recorrer a sistemas de armazenamento de energia.

Neste trabalho, foi feita uma breve revisão dos sistemas atuais com foco nas Baterias de Carnot, cujas características de operação, longa duração de vida e baixa pegada ambiental as tornam competitivas para armazenamento de energia diário; um modelo transiente foi desenvolvido para simular a operação completa de uma Bateria de Carnot que utiliza bombas de calor de compressão de vapor e ciclos orgânicos de Rankine conjuntamente com um armazenamento térmico sensível, foram identificados parâmetros de performance interessantes, e uma otimização foi realizada recorrendo a um equilíbrio entre custos e performance através do teste de 25 configurações de *storage spread* e *pinch point* dos permutadores.

Concluiu-se que as maiores dispersões de temperatura do armazenamento térmico e os maiores *pinch points* levam a menores custos, visto que reduzem o tamanho do tanque de água bem como dos permutadores, e a pior performance pois criam gradientes de temperatura desfavoráveis para a bomba de calor e o motor térmico.

Uma fronteira de Pareto foi identificada, constituída por 10 configurações que otimizam um critério ou um equilíbrio de dois ou mais critérios, e foram tiradas conclusões quanto à aplicabilidade de cada configuração.

Palavras-chave: Armazenamento de Energia Elétrica, Bateria de Carnot, *Pumped Thermal Energy Storage*, Ciclo de Compressão de Vapor, Ciclo de Rankine Orgânico

Contents

LIST OF FIGURES

LIST OF TABLES

LIST OF SIMBOLS AND ACRONYMS

List of Symbols

$\boldsymbol{\varepsilon_{rt}}$ – Roundtrip Efficiency

η – Efficiency

η_s – Isentropic Efficiency

k – Kinetic Energy

I – Moment of Inertia

ω – Angular Velocity

w – Specific Work

q – Specific Heat Energy

h – Specific Enthalpy

U – Heat Transfer Coefficient

R – Thermal Resistance

$\dot{Q}$ – Heat Transfer Rate

$\dot{m}$ – Mass Flow Rate

A – Heat Transfer Area

T – Temperature

t – Time

E – Energy

c_p – Specific Heat Capacity

Acronyms/Abbreviations

IPCC – Intergovernmental Panel on Climate Change

PNEC – Plano Nacional para a Energia e Clima

RNC – Roteiro para a Neutralidade Carbónica

PV – Photovoltaic

ESS – Energy Storage System

VRE – Variable Renewable Energy

EES – Electric Energy Storage

TES – Thermal Energy Storage

PHS – Pumped Hydro Storage

CAES – Compressed Air Energy Storage

SMES – Superconducting Magnetic Energy Storage

CSP – Concentrating Solar Power

WTES – Wind Thermal Energy Storage

CB – Carnot Battery

HT – High Temperature

LT – Low Temperature

PTES – Pumped Thermal Energy Storage

HP – Heat Pump

HE – Heat Engine

VCHP – Vapour Compression Heat Pump

RC – Rankine Cycle

ORC – Organic Rankine Cycle

COP – Coefficient of Performance

TI-PTES – Thermally Integrated Pumped Thermal Energy Storage

1. CONTEXTUALIZATION AND MOTIVATION

According to the IPCC (Intergovernmental Panel for Climate Change), human-induced warming has already reached approximately 1ºC, in 2017. If all human emissions were to be immediately reduced to zero, it's estimated that the total rise in temperature in the time scale of a century would fall under 1.5ºC, in relation to pre-industrial levels. The Paris Agreement has set a goal to limit this global temperature rise to 2ºC, and preferably to keep it under 1.5ºC, as this would substantially reduce the effects of climate change in relation to a future in which no action is taken.

The Portuguese *PNEC 2030 (Plano Nacional de Energia e Clima – National Plan for Energy and Climate)*, regarding national goals and policies for energy use in the 2021-2030 decade, states that the most significant emissions reduction should be felt in the current decade, and that the strongest decarbonization efforts are to be made in the energy, transportation, and residential/service sectors. In the energy sector, emissions reductions are to be achieved mainly by using renewable generation, with the biggest bets being placed on hydro power, wind, and solar photovoltaic (PV). In the industrial, transportation, and residential/services sectors, the main strategy for emissions reduction is to resort to higher shares of electric energy.

Additionally, according to the *RNC2050 (Roteiro para a Neutralidade Carbónica – Roadmap for Carbon Neutrality)*, a long-term plan for achieving net-zero emissions by 2050, the biggest drivers for decarbonization of the energy sector are the use of renewables, increased energy efficiency (which translates into reduced demand from sources), electrification, and new energy vectors such as hydrogen and other synthetic fuels. It states also that the inherent variability of most widespread renewable sources (namely wind and solar PV) creates problems of dispatchability and energy security. The document states that strong grid interconnection with the European Union, smart energy management, and increased usage of Energy Storage Systems (ESS) are key to solving these issues.

This notion is supported by the scientific community, as current papers highlight the necessity for energy storage, often in conjunction with an interconnected and smart grid, to effectively manage the supply variability (on many time scales) resulting from large-scale renewable integration [1]–[4].

1.1. The Challenges of decarbonization in terms of energy storage

The need for inertia in our energy systems is clear – to mitigate variability in supply. However, while most issues caused by integration of Variable Renewable Energy (VRE) sources fall into this category, the features that characterize each problem vary in terms of power requirement, storage duration, discharge time, response time, and other technical characteristics.

Each case is distinct and must be carefully analyzed so that an appropriate solution may be selected, however, we may roughly divide the main challenges of renewable integration into a few types and characterize them in terms of the requirements listed above.

1.1.1. Load Shifting and Seasonal Storage

Because of the largely uncontrollable nature of VREs, supply of electric energy will rarely match demand – In these cases, we often require storage systems to shift the supply to more favorable periods of time, to satisfy demand and prevent curtailing. This is the most important application of energy storage in the context of decarbonization.

The needed storage duration will vary depending on the characteristics of the generation source, but it should fit roughly in the time scale of its natural variation; this can range from a few hours – the case for solar variation [3] – to days, weeks or even months – the typical long-term variation in wind speeds [2], [3].

Power requirements must also match the generation source, in the order of 10-100 MW for grid scale applications, with lower values for localized/consumer-scale situations.

Maximum response times must be in the scale of minutes, and the capacity should be sufficient to absorb excess power and satisfy demand. For large scale applications with seasonal storage, it may reach values in the order of 100-1000 MWh [1].

1.1.2. Power Quality

At a very small time scale, fluctuations in supply and demand can affect the properties of electric current, such as voltage and frequency [2]. To maintain the desired qualities of supplied energy, storage systems are often used. For these applications, storage duration and capacity may be limited, however power and response time are critical parameters, as power

(in the order of kW to several MW, depending on the scale of consumption) is to be processed almost instantaneously, in the order of milliseconds.

1.1.3. Transmission and Distribution Management

With increasing loads being placed on electric grids, bottlenecks may appear in periods of peak consumption. Alongside other measures, such as economic incentives for shifting consumption, storage systems may be used to absorb excess loads and delay costly investments into power grids.

The storage duration required should fit the variations in demand (several hours). Power and capacity requirements depend on the scale of application, but are similar to those of grid-scale load-shifting. Response times up to a few minutes should be sufficient.

1.1.4. Backup Power

At the consumer scale, energy storage may be desired to maintain an uninterrupted power supply in case of an outage. In this case, power requirements should match the consumption load (from a few kW to tens of MW), and storage capacity and duration should match the expected outage period (usually up to a few hours, with enough capacity to satisfy power requirements over this period – up to the order of 10 MWh). Response time is a critical parameter as the grid power must be replaced immediately – a response in the order of milliseconds is ideal.

1.1.5. Transportation

To effectively replace fossil fuels in the transportation industry, the storage medium to be used must have high specific energies and energy densities, along with a quick response time. Power-To-Fuel technologies that produce fuels compatible with current fossil-based systems are a good solution for this sector [1].

1.2. Classification of Existing Technologies

Currently, a wide variety of storage solutions exist, with various approaches to energy conversion reflected in their operating principles.

Energy may be stored in various forms, the most common being chemical potential, magnetic fields, electric fields, pressurized gas, gravitational potential, thermal energy, and synthetic fuels [1], [2].

In the literature, the classification of storage systems varies slightly from author to author, as the mechanisms employed by storage systems, as well as the perspectives from which we classify them, are diverse.

In [1], A.B. Gallo *et al.* classify storage systems by their output and the intermediate storage form, regardless of input, which is electricity or thermal energy. Systems which output electric energy are classified as Electric Energy Storage (EES), and systems which output thermal energy are classified as Thermal Energy Storage (TES). In the author's opinion, this classification is somewhat flawed, as it doesn't allow for systems to be viewed from a multisectoral approach (for example, thermal systems which can simultaneously output heat and electricity, would be hard to classify using this scheme). This classification also depends on the system boundaries considered – A thermal storage tank fed by electrical resistance may be seen as TES if the boundary is drawn at the output of the tank, but if coupled to a heat engine for electricity production it may be seen as an EES – hence it may lead to misinterpretation.

Other authors have different approaches to classifying systems, but many simply classify systems by the type of energy stored. The main categories usually considered are electrical, electrochemical, mechanical, thermal, and chemical, depending on the storage mechanism [3], [4]. This work will consider this classification scheme. A short description of each technology will be given and general values provided for their characteristics.

Table 1.1 presents a brief classification of some fundamental systems.

Table 1.1. Classifications of ESS

Stored Energy	Storage Mechanisms	Examples
Electric	Electric and magnetic fields	Supercapacitors, SMES
Electrochemical	Reversible chemical reactions	Conventional Batteries, Flow Batteries, High-Temperature Batteries, Metal-Air Batteries
Mechanical	Gas pressure, gravitational potential, kinetic energy	CAES, PHS, Flywheel
Thermal	Heat capacity of a material, latent heat of phase change, endothermal and exothermal reactions	TES (Sensible, Latent, Thermochemical)
Chemical	Production of synthetic fuels	P2G, P2L

1.2.1. Pumped Hydro Storage (PHS)

Pumped Hydro Storage, displayed in Figure 1.1, exploits the change in elevation between reservoirs of water in order to store energy in the form of gravitational potential. In charge mode, water is moved to a high elevation, increasing its potential energy, and in discharge mode this energy is converted into kinetic energy as the water flows back to the lower reservoir, passing through a turbine which generates electricity.

PHS has a good degree of maturity and commercial exploitation [1], [5], and is suitable for high power and high energy applications. It has low energy costs and a relatively high efficiency, however it comes with the downsides of high environmental impact, and geographical restrictions. Additionally, this technology is becoming increasingly difficult to exploit, as in most developed countries the potential for new installations is nearly exhausted [5], [6].

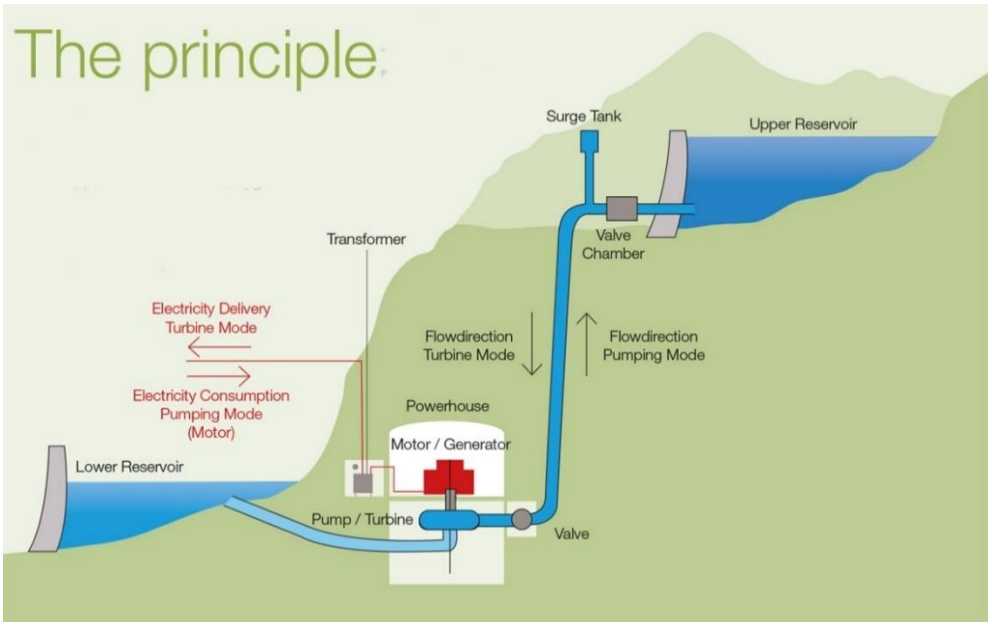

Figure 1.1. Working principle of a PHS system [7]

1.2.2. Compressed Air Energy Storage (CAES)

CAES is a system which stores energy in the form of gas pressure. In the charging process, air is compressed and sent into an underground reservoir, and in the discharge process this pressurized air is expanded in a gas turbine to generate electricity. The variants of this technology mostly differ by their handling of the heat which is added to the air upon compression as shown in Figure 1.2. In Diabatic CAES, this heat is removed to the atmosphere, and the air is re-heated upon expansion, Adiabatic CAES stores this heat in a thermal storage, returning it to the air upon expansion, and in Isothermal CAES a water spray is used to maintain nearly constant compression and expansion temperatures. In all cases, the air may be kept at a constant pressure (underground or in above-ground containers), or at constant volume (inside underwater bags) [1].

These systems benefit from a very low environmental impact (if fossil fuel use is avoided), and excellent power and storage capacities. However, they suffer from geographical limitations, as they most often require an underground cavern for storage.

Figure 1.2 schematizes the operation of Diabatic and Adiabatic CAES.

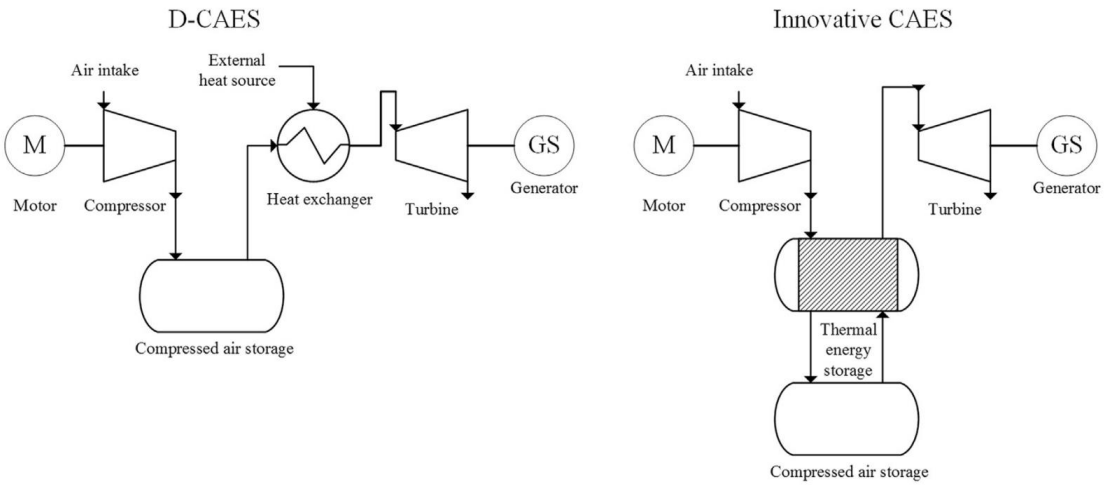

Figure 1.2. Schematic illustration of Diabatic and Adiabatic CAES [1]

1.2.3. Flywheel Energy Storage

In flywheels, storage takes the form of kinetic energy of a rotating mass. This is one of the simplest forms of storage, where the total energy stored can be obtained from the following expression:

$$k = \frac{1}{2} \cdot I \cdot \omega^2, \tag{1.1}$$

Where k is the kinetic energy associated with the mass, I is its moment of inertia, and ω is its angular velocity.

For the charge process, an electric motor draws electric energy to accelerate the flywheel rotor, converting it to kinetic. To discharge, the same motor now acts as a generator, decelerating the mass and converting its kinetic energy into electric energy. The rotor is usually made of steel, a cheap and recyclable material, for low-speed applications (<10,000 rpm), or a composite material for high-speed applications (<100,000 rpm) [1].

Even with the use of magnetic bearings and low-friction atmospheres, these systems experience extremely high self-discharge rates, making them unsuitable for long-term storage [1]. However, their quick response and high power ratings make them excellent for applications that require fast bursts of energy, such as power regulation.

In Figure 1.3, a detailed illustration of a flywheel system is shown.

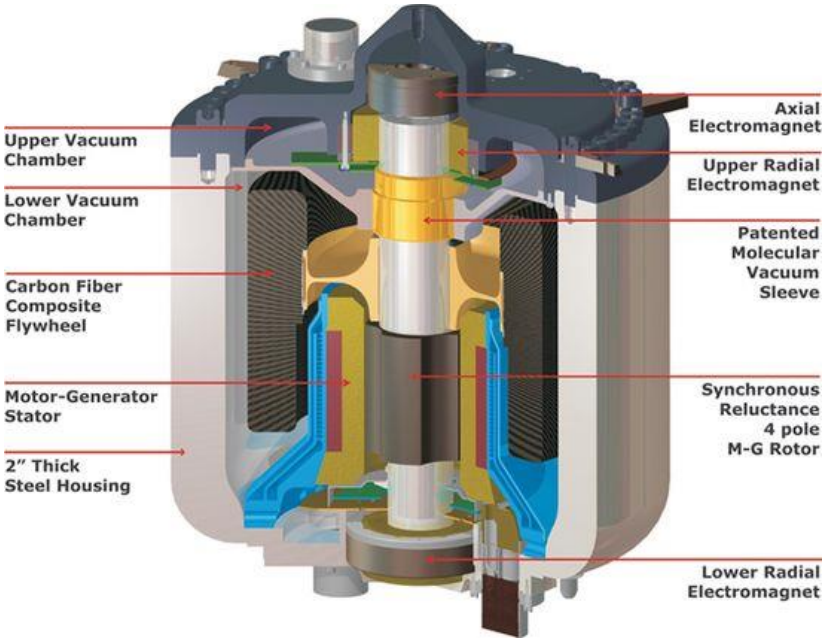

Figure 1.3. Illustration of a Flywheel Storage System [8]

1.2.4. Electrochemical Batteries

Electrochemical batteries store energy in the form of a reversible chemical reaction – in the discharge process, a redox reaction generates an electric current between the two electrodes. For charging, the reaction is reversed, absorbing electric current. Due to the speed of the reactions, the response time of these batteries is nearly instantaneous, making them adequate for applications requiring some agility, such as power quality and managing quick

changes in renewable generation; however, this kind of battery generally suffers from environmental issues, high costs, and limited cycle life.

1.2.4.1. Conventional Batteries

In the realm of conventional batteries, the most commonly used are lead-acid, lithium-ion, nickel-cadmium and nickel-metal hydride. These batteries use solid anodes and cathodes immersed in an electrolyte, which serves as a conducting medium for the chemical reactions that release and absorb current in discharge and charge modes, respectively.

Lead-acid batteries are the oldest type, having been in use for over 150 years, and offer acceptable efficiencies and low costs, with the disadvantages of a limited service life and environmental issues, as the lead is quite toxic.

Lithium-ion batteries are more recent, with their first commercial application in 1991, and they offer excellent power/energy densities and efficiencies. Currently their main drawback is cost, but further development in this technology is expected to drive prices down.

Nickel-cadmium and nickel-metal hydride batteries are a mature technology which presents advantages over lead-acid batteries, such as a longer cycle life and higher specific energy, with the drawbacks of toxicity issues and a memory effect which compromises their capacity for cycles at a low depth of discharge [1].

Figure 1.4 presents a basic illustration of a Lithium-Ion battery.

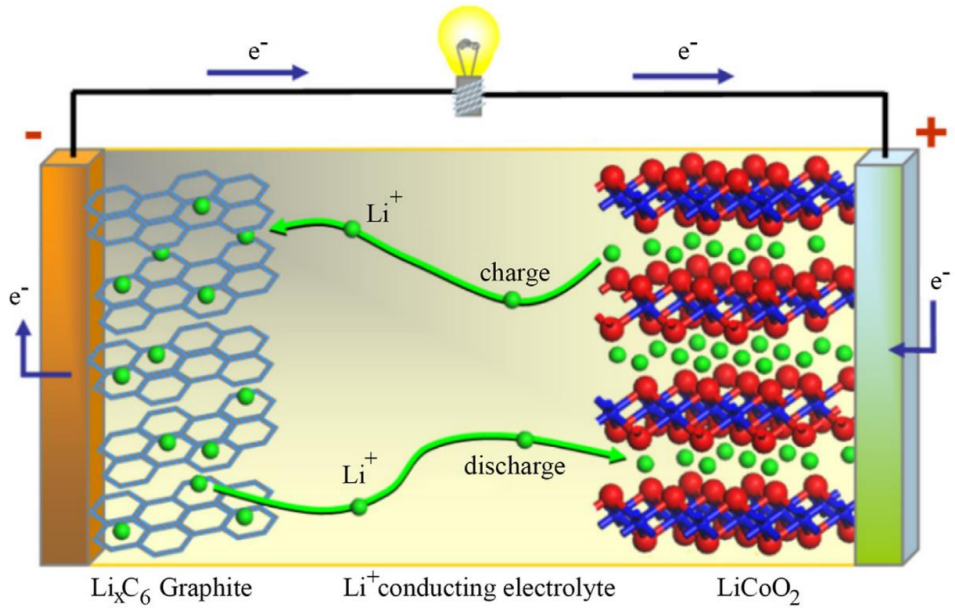

Figure 1.4. Illustration of a lithium cobalt oxide battery [1]

1.2.4.2. Flow Batteries

In principle, flow batteries work similarly to conventional batteries. However, flow batteries operate by pumping two separate electrolyte solutions (equivalent to the positive and negative electrodes in a conventional battery) through a circuit, on both sides of an ion-selective membrane, as shown in Figure 1.5. In discharge mode, ions flow through the membrane, releasing an electric current to an exterior circuit.

The main advantage of these batteries is that power and energy capacity can be designed separately, as power depends on the size of the membrane, and capacity depends on the volume of the liquid solutions.

This type of battery offers low energy densities and moderate-high efficiencies. However, its self-discharge is extremely low, and its lifetime quite high [1].

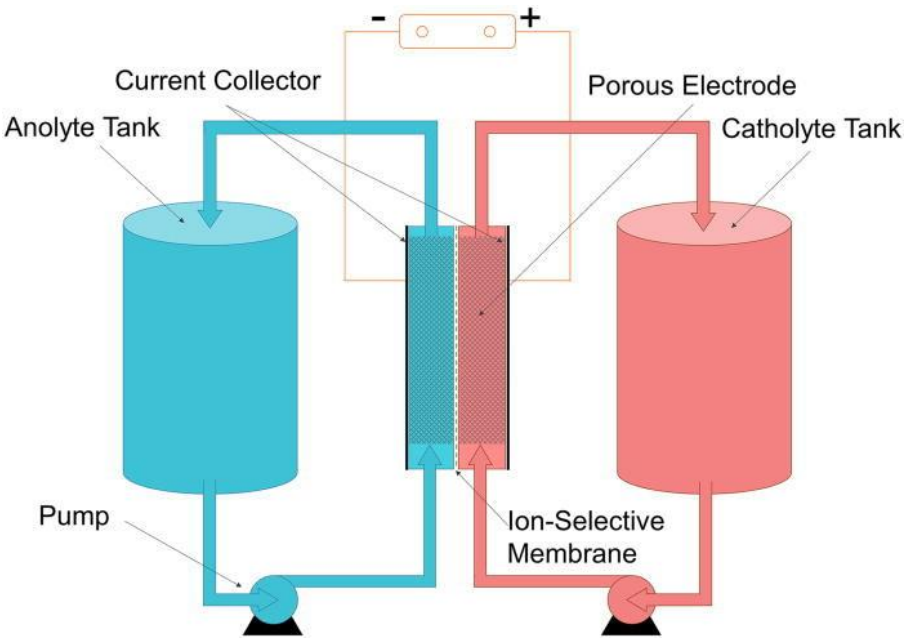

Figure 1.5. Functioning principle of flow batteries [9]

1.2.4.3. High Temperature Batteries

High Temperature (HT) batteries rely on molten electrode materials (sulfur and sodium, or sulfur and nickel-chloride, thus they must be maintained at high temperatures to prevent phase change.

The charge reaction of these batteries is endothermic, with a small decrease in temperature, and the discharge reaction is exothermic. As the discharge releases more heat than the charge process absorbs, frequent cycling will minimize self-discharge losses in this

type of battery, making them adequate for applications with a high number of cycles. For long standby periods, these batteries experience higher levels of self-discharge.

This kind of battery has good specific energies and high efficiencies, as well as a long lifetime. In the case of Na-S batteries, exhibited in Figure 1.6, the materials used are cheap and recyclable, with the main concern being flammability issues because of the molten sodium [1].

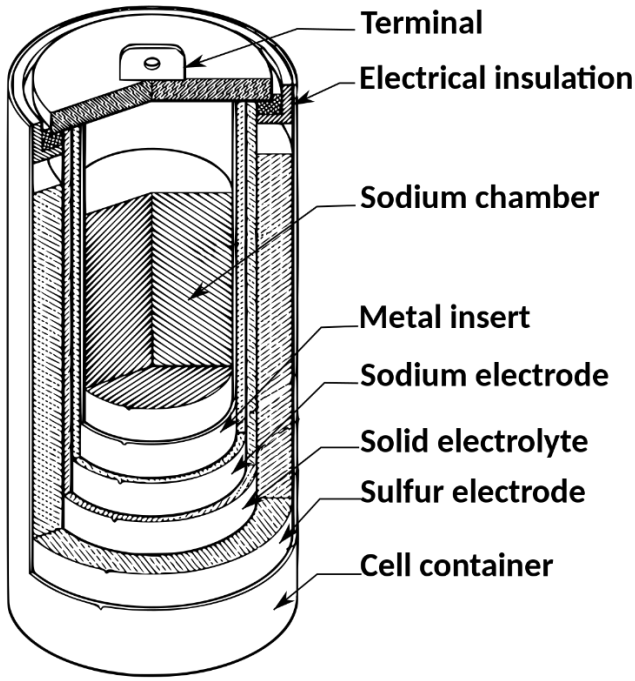

Figure 1.6. Illustration of a Na-S cell [10]

1.2.5. Supercapacitors

Supercapacitors are a development of regular capacitors, which store energy by accumulation of positive and negative charges on either side of a dielectric, inducing an electric field.

These devices can be cycled very quickly, and achieve very long cycle lives [1]. Supercapacitors have high energy densities and high efficiencies compared to capacitors, with their main advantages being a very high power density and quick response times, making them adequate for power regulation.

Figure 1.7 shows a 3.0 Wh supercapacitor.

Figure 1.7. Image of a supercapacitor [11]

1.2.6. Superconducting Magnetic Energy Storage (SMES)

SMES systems store energy in the form of a magnetic field, induced by a dynamic electric field passed through a coil. In SMES, the coil is made of a superconducting material which is kept below its superconducting critical temperature, allowing current to pass through it with almost no resistance losses, thus minimizing self-discharge [1]. A simplified schematic of SMES is shown in Figure 1.8.

These systems have high efficiencies, very fast response times, and high power densities, making them well suited for high frequency and high power applications such as power quality regulation.

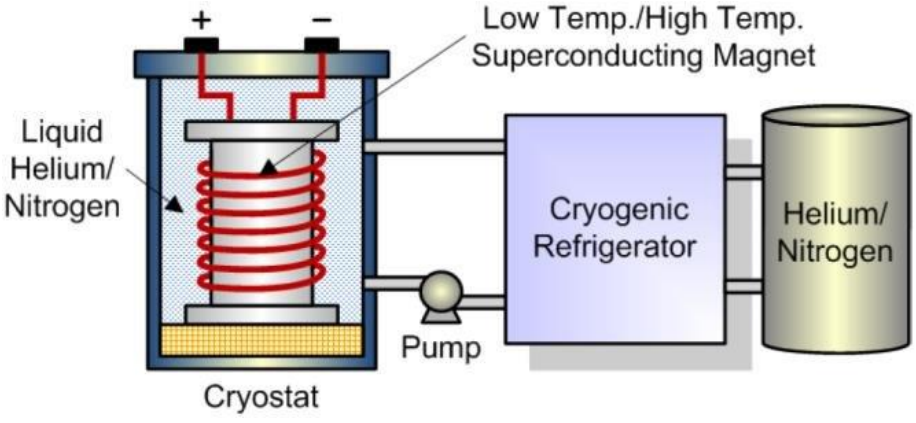

Figure 1.8. Schematic representation of a SMES [12]

1.2.7. Thermal Energy Storage

These systems store energy in the heat capacity of a solid or liquid material (Sensible Heat Storage), the latent heat of a phase change (Latent Heat Storage) or in a reversible thermochemical reaction (Thermochemical Storage).

These systems can also vary by the method through which the storage medium is charged. Concentrated Solar Power (CSP) plants, if coupled with thermal storage, use solar radiation to heat a storage medium, which can then discharge to a heat engine for electricity production [13]. Another possibility is Wind-powered Thermal Energy System (WTES), in which wind power is converted directly to heat, which is stored in a TES and later used to power a heat engine [13]. The thermal storage may also be charged using electricity, in which case the whole system may be designated a Carnot Battery, and if a heat pump is used to charge the system it is designated a Pumped Thermal Electricity Storage (PTES), so long as the heat is used to produce electricity in the discharge phase.

The Carnot Battery presents several advantages that make it competitive with other forms of ESS, mainly in terms of environmental impact, flexibility and efficiency, and so it will be the focus of this work.

To conclude this section, key features of the various ESS that were studied are summarized in Table 1.2 and Table 1.3 .

Table 1.2. Summary of most common Energy Storage Systems

Technology	Source	Power [MW]	Energy [MWh]	Discharge Time	Response Time	Self-Discharge (%/day)	Suitable Storage Duration	Roundtrip Efficiency (%)	Lifetime (years)
PHS	[1]	100-5000+	1000+	1-24+ h	~3 min	0.005-0.02	h-month	65-85	30-60
	[14]	10-5000		1-24+ h	s-2 min		mid-long term		
CAES	[1]	0.1-1000+	1-1000+	1-24+ h	1-10 min	0.003-1	h-month	40-95	20-40
	[14]	5-1000		1-24+ h	1-15 min		mid-long term		
Flywheel	[1]	0.1-10	0.01-5	ms-s	ms-s	55-100	s-min	75-95	15-20
	[14]	0-20		ms-min	4 ms-s		s-short term		
Conventional Batteries	[1]	0.001-50	10^{-5}-100	s-h	ms	0.033-1.2	min-day	60-95	5-20
	[14]	0-100		s-h	ms-s	0-0.83	short-long term	50-98	5-20
Flow Batteries	[1]	0.005-15	0.01-10+	s-10 h	ms	0.2-0.24	h-month	57-85	5-15
	[14]	0.05-15		sec-10 h	s-10 min	0.2-0.24	long term	60-85	5-20
HT Batteries	[1]	0.001-50	0.12-600	s-h	ms	0.05-20	s-h	70-90	10-15
	[14]	0-34		s-h	s-2 min	0.05-20	mid-long term	70-92.5	5-20
Supercapacitors	[1]	0.001-10	10^{-6}-10^{-2}	ms-h	ms	20-40	s-h	85-95	10-20
	[14]	0-10		ms-h	<10 ms	5-40	short term	60-99	8-20
SMES	[1]	0.01-10	10^{-4}-0.1	ms-min	ms	10-15	min-h	80-90	15-20
	[14]	0.1-10		ms-1 min	<100 ms	10-15	short term	80-98	20-30
PTES	[1]	0.5-10+	0.5-60+	1-6+ h	<1 min	1	h-month	70-80	25

Table 1.3. Summary of most common Energy Storage Systems (cont.)

Technology	Source	Power Density [kW/m^3]	Specific Power [W/kg]	Energy Density [kWh/m^3]	Specific Energy [Wh/kg]	Capital Power Cost ($/kW)	Capital Energy Cost ($/kWh)	Maturity	Applications
PHS	[1]	-	-	0.5-1.5	0.5-1.5	600-2000	5-100	Mature	Load-Shift
	[14]	0.5-1.5		0.5-2		2500-4300	5-271	Commercialized-Matured	
CAES	[1]	-	-	3-12	30-60	400-2000	2-200	R&D-Commercial	Load-Shift
	[14]	0.5-10		0.4-20		400-1628	2-271	Commercializing	
Flywheel	[1]	1000-2000	400-1500	20-80	5-100	250-350	1000-5000	Commercial	Power Quality
	[14]	800-2000		20-80		250-380	500-14,000	Matured-Commercializing	
Conventional Batteries	[1]	10-10,000	75-2000	50-500	20-250	300-4000	200-2500	Commercial-Mature	Load-Shift, Power Quality, Backup Power, Transportation, T&D Management
	[14]	7.8-5000	25-600	15-500	15-207	200-4342	54-2500	Demonstration-Commercialized	
Flow Batteries	[1]	0.2-25	45-166	150-250	10-85	330-2500	120-1000	Demonstration-Commercial	Load-Shift, Power Quality, Backup Power, T&D Management
	[14]	0.5-34	1.31-166	10-70	10-54	175-4500	110-2000	Developing-Commercializing	
HT Batteries	[1]	120-300	150-230	85-240	85-240	~400-3000	300-1000	Commercial	Load-Shift, Power Quality, Backup Power, T&D Management
	[14]	3.5-500	150-230	100-280	100-240	150-3256	100-543	Proven-Commercialized	
Supercapacitors	[1]	100,000	500-5000	10-30	2.5-50	100-360	300-2000	Demonstration-Pre-Commercial	Power Quality
	[14]	1000-5000	500-10,000	1-35	0.5-22	100-480	300-2000	Demonstration-Commercial	
SMES	[1]	1000-4000	500-2000	0.2-2.5	0.5-5	200-350	1000-10,000	Demonstration-Pre-Commercial	Power Quality
	[14]	300-4000	500-2000	0.2-13.8	1-75	200-489	1085-10854	Commercializing	
PTES	[1]	-	-	~110-170	~50-140	~600	~60	R&D-Pre-Commercial	Load-Shift, T&D Management

2. CARNOT BATTERIES

According to O. Dumont *et al.* [5], a Carnot Battery (CB) is defined as an EES technology where there is always an electric input, and an electric output. A thermal input may be used to improve the performance of the CB; however, its primary purpose remains the storage of electric energy. Similarly, the battery may output useful thermal energy, but the electric output must be comparable with the electric input.

Carnot Batteries work by establishing a thermal gradient between a high temperature (HT) reservoir and a low temperature (LT) reservoir. Electric energy is used to charge the system by forcing heat flow against the natural gradient, thus storing thermal exergy. In the discharge phase, the heat flows from the hot environment to the cold one, and this flow is used to produce work in a heat engine. The general functioning principle of Carnot Batteries is shown in Figure 2.1

In practice, the reservoirs may be physical ones, such as water tanks or solid materials, or their role may be taken up by the environment (for example, the ambient air). Similarly, electric heat pumps or resistance heaters may be used for charging, and any heat engine (Rankine, Brayton, others) or even a thermoelectric generator may be used for discharging.

Carnot Batteries offer roundtrip efficiencies (ε_{rt}) in a wide range depending on their boundary conditions [5], [15]–[17], low energy costs [1][5], and high lifetimes [1][5]. These systems are mostly competitive for electricity storage on the scale of several hours, in situations that demand low Power/Capacity (kW/kWh) ratios, with values of 1/4 h^{-1} and lower [5]. They have a very low environmental impact, and no dependence on geographical conditions [1][5], making them a suitable competitor to PHS and CAES, whose geographical constraints pose a considerable limit to their exploitability on a large scale. For local, small scale implementations, Carnot Batteries may also present an adequate replacement for chemical batteries, which are often expensive and environmentally unsafe.

Additionally, an important advantage of Carnot Batteries is the ability to integrate additional thermal reservoirs (such as industrial waste heat), which act as additional exergy sources [5]. This thermal integration increases the ε_{rt} of the system, potentially to values greater than unity (>100%), by decreasing the work input or increasing the work output.

In Table 2.1 a brief summary is given of the technical characteristics of some different Carnot battery technologies. Additionally, in [5], a continuously updated table of Carnot Battery Prototypes is presented, which may be consulted for information about existing projects.

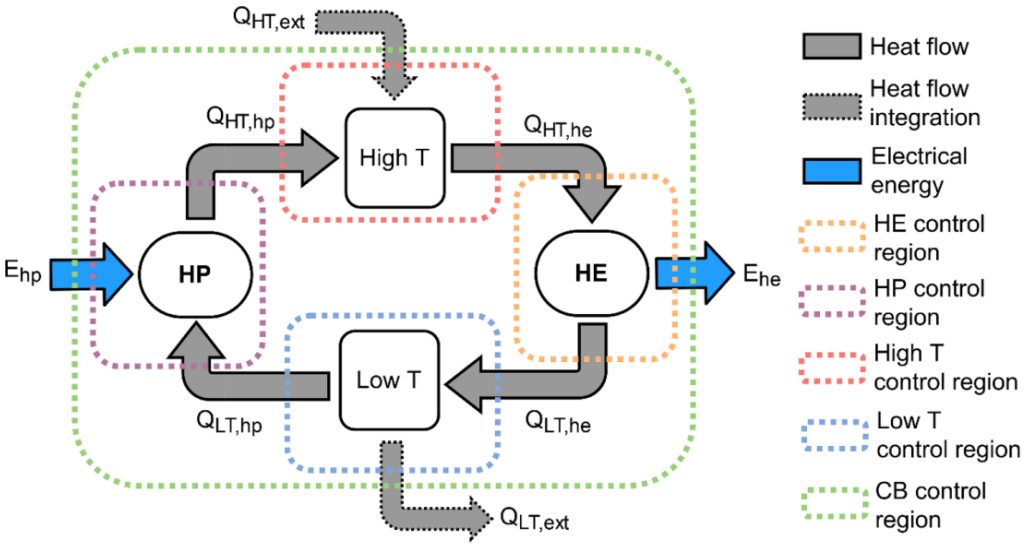

Figure 2.1. Generic representation of a Carnot Battery (HE – Heat Engine; HP – Heat Pump) [5]

Table 2.1. Technical summary of Carnot Battery technologies (adapted from [5])

Cycle	Brayton Cycle	Electrical heater and Rankine Cycle	Heat Pump and Rankine Cycle
Power [MW]	Up to 100	Up to 100	Up to 10*
Energy [MWh]	Up to 400	Up to 400	Up to 40*
Temp [°C]	[-70:1000]	Up to 750	Up to 150
Compactness [kW/m^3]	25	~4	[0.05–1.72]
Compactness [kWh/m^3]	200	~36	[0.2–207]
Self-discharge	medium	Very low	[30–73]
ε_{rt} [%]	[60-70]	[12-55]	[70-150]**
Price [$/kW]	[395-875]	~376	[272–468]
Price [$/kWh]	[55–198]	~94	[68–117]
Estimated TRL	5	9	7
Typical fluids	Argon, Air	Water	R1233zd(E),CO2, NH3, water

*Possible to extend by association in series
**Thermally integrated

2.1. Pumped Thermal Electricity Storage

If a heat pump is used to charge the thermal storage, the system is designated Pumped Thermal Electricity Storage. These systems may use Brayton heat pumps (HP) with Brayton heat engines (HE), Vapour Compression Heat Pumps (VCHP) in conjunction with Rankine Cycles (RC), or Brayton heat pumps with Rankine Cycles [6].

The presence of a heat pump for the charge cycle is advantageous if the Coefficient of Performance (COP) is higher than one, as the roundtrip efficiency of a PTES is generally the product of the COP with the HE efficiency (if thermal storage efficiency is not considered).

The use of a heat pump brings advantages in terms of thermal integration, as it can increase the performance of the heat pump and/or the heat engine. This thermal integration allows an increase in efficiency without complex modifications to the thermodynamic cycles and makes the PTES more flexible, as it may now receive two inputs (electric and thermal) instead of just one – in this sense, Thermally Integrated PTES (TI-PTES) may be seen as a hybrid energy storage and waste heat power plant.

Two thermal integration options generally considered are Hot TI-PTES and Cold TI-PTES.

In Hot TI-PTES, the TES is hotter than the environment, and the waste heat is used in the charge phase to reduce the temperature lift (the difference between the high and low temperatures) of the heat pump by increasing the evaporation temperature, thus increasing the COP; in the discharge phase, the ORC efficiency is unchanged [6].

In Cold TI-PTES, the TES is colder than the environment, and the heat pump now acts as a cooling machine, removing heat from the cold TES. The waste heat is exploited in the discharge phase, increasing the temperature gradient of the heat engine as it discharges to the cold TES. This style of waste heat integration has no effect on the COP, but it increases the HE efficiency [6].

Theoretically, the efficiency of Hot TI-PTES is always higher than that of Cold TIP-TES [5], [6], however the cold system offers the advantage of a cheap, safe, and reliable Phase Change Material (PCM), as the water-ice transition can be used for exergy storage.

Table 2.2 summarizes key technical features of some PTES studies that were reviewed, and Figure 2.2 shows the working principle of PTES with and without thermal integration.

Following this introduction, some configurations of PTES will be discussed.

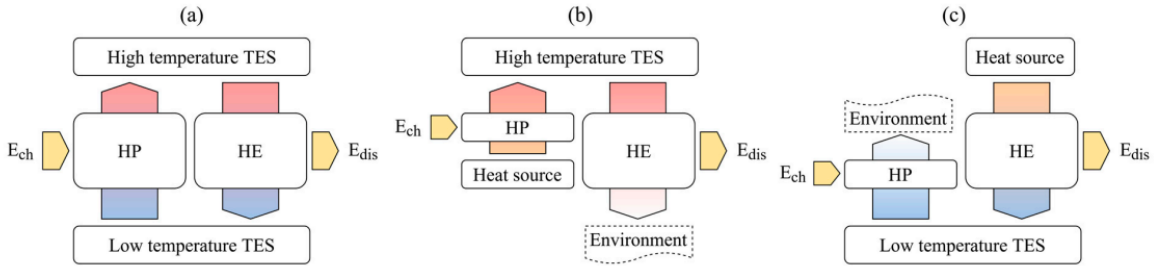

Figure 2.2. PTES working principle. (**a**) Standalone PTES; (**b**) Hot TI-PTES; (**c**) Cold TI-PTES [6]

Table 2.2. Technical summary of Reviewed PTES studies

Title	Year	Author	Cycle	Thermal Integration	Power [kWel]	P2P (%)	Tsource [°C]	Tsink [°C]	Storage	Tstorage [°C]	Working Fluid	Isentropic efficiencies	Type of study
Carnot battery: Simulation and design of a reversible heat pump-organic Rankine cycle pilot plant	2021	Eppinger *et al.*	HP/ORC	Yes (simulated)	14 (compressor)	59	-	-	Sensible	90-120	R1233zd(E)	0.7 (comp.) 0.7 (exp.) 0.8 (pump)	Theoretical
Experimental Investigation Of A Thermally Integrated Carnot Battery Using A Reversible Heat Pump/ Organic Rankine Cycle	2021	Dumont *et al.*	HP/ORC, reversible	Yes	1.3 (compressor)	72.5	-	-	Sensible	110 (max)	R1233zd	Up to 0.75 (comp.) Up to 0.64 (exp.)	Experimental
Reversible Heat Pump–Organic Rankine Cycle Systems for the Storage of Renewable Electricity	2018	Staub *et al.*	HP/ORC	Yes	100 (compressor)	63-70	90	40	Sensible	110-160	R365mfc	0.7 (comp.) 0.7 (exp.)	Theoretical
Design aspects of a reversible heat pump - Organic rankine cycle pilot plant for energy storage	2020	Steger *et al.*	HP/ORC	Yes	15 (input)	59	90	40	Sensible	90-120	R1233zd(E)	0.7 (comp.) 0.7 (exp.)	Theoretical
Pumped thermal energy storage (PTES) as smart sector-coupling technology for heat and electricity	2019	Steinmann *et al.*	HP/ORC	Yes	-	20-125	40-100	15-40	Latent	132	Butene	-	Theoretical
Organic flash cycles in Rankine-based Carnot batteries with large storage temperature spreads	2022	Weitzer *et al.*	HP/ORC/OFC, Reversible HP/ORC	Yes/No	-	30-140 87.7	20-30-90	30 (Tcond)	Sensible	90-120	R245fa	0.8 (comp.) 0.8 (exp.) 0.8 (pump) 0.7 (2-phase exp.)	Theoretical

2.1.1. Brayton

Brayton PTES is usually comprised of a Brayton heat pump, based on the inverse Brayton cycle, and a Brayton heat engine, typically working between two sensible reservoirs [5]. The typical layout contains two thermal reservoirs and four machines (two compressors and two expanders), however in a reversible system this number could reduce to two [5].

In a Brayton cycle, the working gas is compressed, heated and expanded, and then cooled before the next compression. As the work produced by expansion is greater than the work used in compression, the expander drives the compressor with a net positive work output (as with any heat engine, the driving force is a temperature gradient between the two reservoirs) – this is the cycle followed in the discharge process. For charging, the inverse process occurs – the gas is heated and compressed, drawing heat from the LT reservoir, and then cooled, storing heat in the HT reservoir, followed by expansion [5].

These systems typically work between very low and very high temperatures – [5] cites a system that works between -70°C and 1000°C – making Brayton PTES suitable for cryogenic waste integration, but poorly suited for typical waste heat integration. However, practical and technical considerations tend to limit this temperature range [5].

The literature reports roundtrip efficiencies around 60-70%, however these values are highly sensitive to machine polytropic performance, for which optimistic values have mostly been considered so far [5].

Figure 2.3 shows the working principle of a Brayton Cycle heat pump.

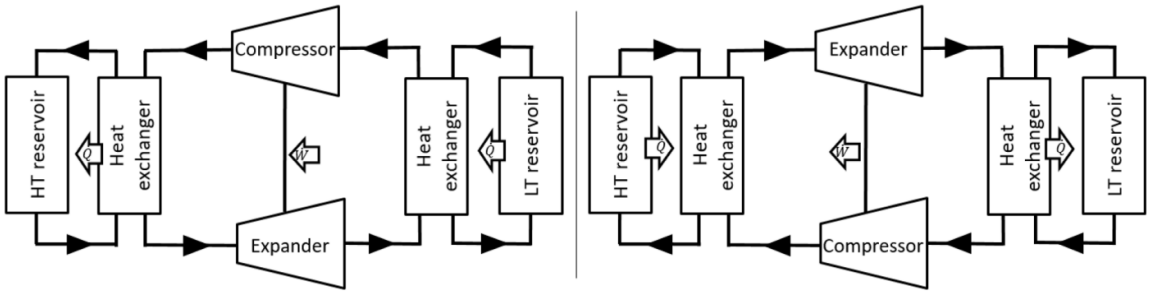

Figure 2.3. Reversible Brayton Cycle (left: charge, right: discharge) [5]

2.1.2. Heat Pump/Rankine Cycle (HP/RC)

HP/RC systems combine Vapour Compression Heat Pumps with Rankine Cycles, where the VCHP charges the reservoirs with thermal exergy, and the Rankine Cycle produces work by harnessing the temperature difference between HT and LT reservoirs.

By comparison with Brayton systems, Rankine-based PTES offers the advantages of high energy density and low temperature operation – these features allow for more compact storage, lower self-discharge, and potentially more efficient integration of waste heat.

The working fluid of choice may be water, CO2, Ammonia, or an organic refrigerant – in the last case, the system is designated Heat Pump/Organic Rankine Cycle (HP/ORC).

One of the advantages of HP/ORC systems is the use of commercially available equipment (pumps, compressors, expanders, heat exchangers, valves), which facilitates their construction [5], [6], [18].

The schematic configuration for HP and ORC systems is shown in Figure 2.4, and the corresponding T-s diagrams in Figure 2.5.

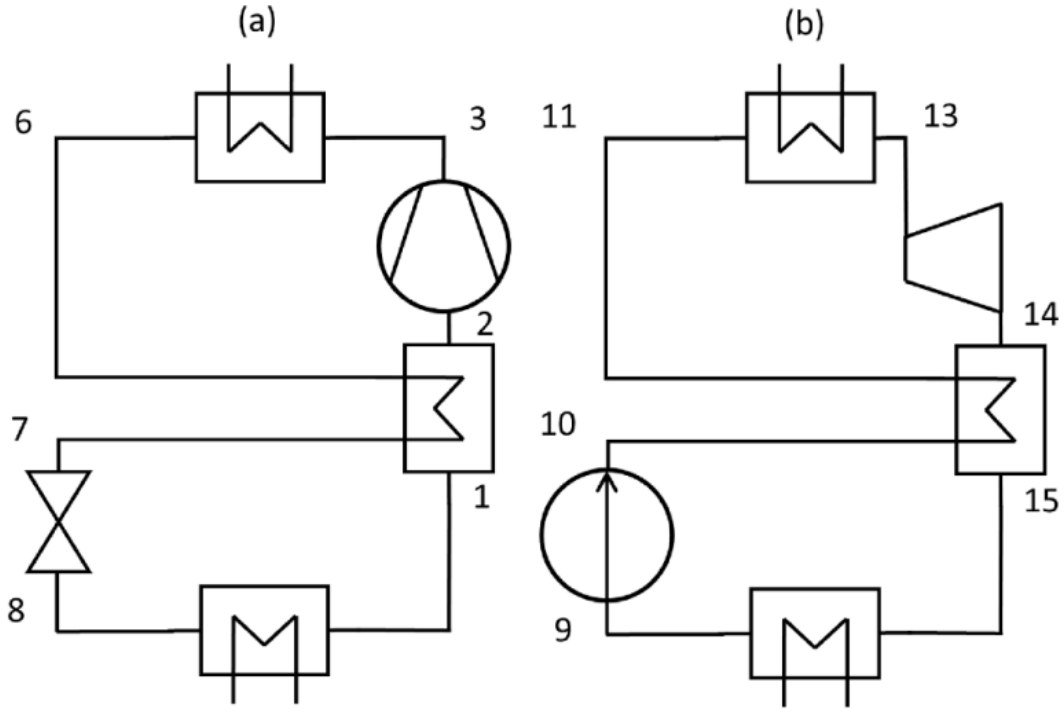

Figure 2.4. Heat pump (**a**) and ORC (**b**) schematic diagrams [12]

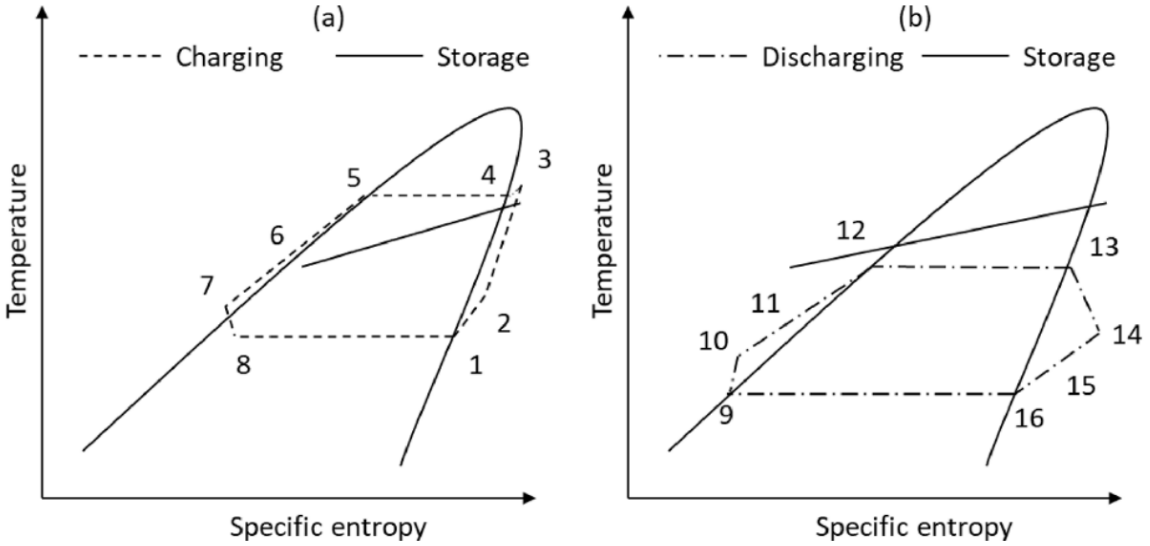

Figure 2.5. Heat pump (**a**) and ORC (**b**) T-s diagrams, with visualization of a latent storage curve [12]

Reversible systems are also of great interest, further simplifying the assembly as the merging of charge and discharge cycles eliminates the need for separate compression and expansion machines, significantly reducing investment costs. This makes reversible systems appealing for small-scale applications (a few kW), as the low costs compensate the difficult optimization, and resulting inefficiency, inherent to these systems – the optimization of either cycle is impossible as the machines have different optimal operation characteristics, however they must work in the same conditions for both cycles [5], [6], [15], [18]–[20]. For larger scales, more complex systems with separate machines are advantageous [6].

A simple reversible machine is schematized in Figure 2.6.

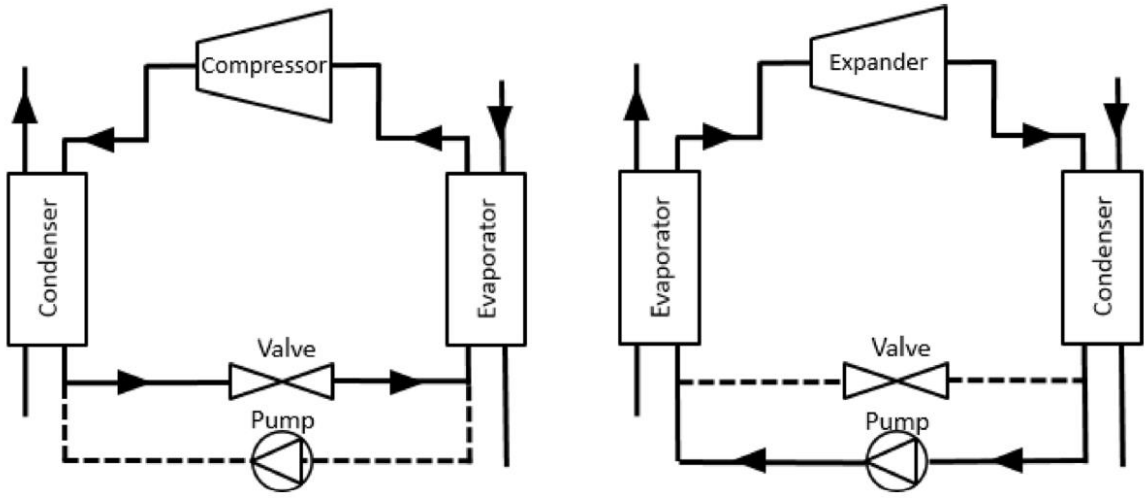

Figure 2.6. Reversible HP/ORC (left: HP mode, right: ORC mode) [5]

The low operating temperatures of HP/ORC systems, generally under 200°C, also allow relatively simple integration of waste heat sources [5], [6], with many studies looking into the optimization of TI-PTES using this architecture [15]–[18]. TI-PTES and similar technologies are usually proposed in the range of 10 kW to 1 MW or lower, making them more suited to distributed storage/generation than to centralized applications – this is consistent with the fact that thermal integration requires planning and optimization on a local scale [6].

3. MATLAB IMPLEMENTATION

For the study of Carnot Battery systems, the HP/ORC architecture was chosen due to its simplicity and practical feasibility, as well as its low temperatures that facilitate thermal integration; this is also one of the most widely studied types of Carnot Battery, so reference values are readily available.

To study the performance of HP/ORC PTES, each thermodynamic cycle was modelled in MATLAB, with resort to the software REFPROP and a MATLAB script to calculate fluid properties. Following that, a transient model was developed to simulate the behaviour of a TES coupled to each cycle.

3.1. Carnot Cycles

A theoretical battery using Carnot cycles provides insight regarding performance in the most ideal circumstances, in the absence of irreversibility. The Carnot efficiency and Carnot COP of the heat engine and heat pump, respectively, depend only on the temperature levels of the hot and cold reservoirs, and are given by equations 3.1 and 3.2:

$$\eta = 1 - \frac{T_H}{T_C}, \text{ and} \tag{3.1}$$

$$\mathrm{COP} = 1 - \frac{T_H}{T_H - T_C}, \tag{3.2}$$

Where η is the HE efficiency, COP is the Coefficient of Performance of the HP in heating mode, and T_H and T_C are the hot and cold reservoir temperatures in Kelvin, respectively.

Additionally, the roundtrip efficiency of the battery is given by the product of the COP with the HE efficiency:

$$\varepsilon_{rt} = \mathrm{COP} \times \eta, \tag{3.3}$$

Using theoretical Carnot values, this is the maximum possible roundtrip efficiency of any Carnot Battery, regardless of the exact nature of the thermodynamic cycles used. It should be noted that without thermal integration – when the same low and high temperatures are used in both machines – the theoretical Carnot efficiency will always be 100%. This is because no irreversibilities are considered to degrade the performance of the cycles.

This model is far too simple for any practical application; however, it can be used to determine the level of optimization of any heat engine or heat pump.

3.2. Simple VCHP/ORC

Initially a simple Carnot Battery consisting of standard heating and power cycles, specifically a simple VCHP and ORC, was simulated. Each cycle consists of four processes, generally two heat exchanges at constant pressure, and two compression/expansion processes.

3.2.1. Simple VCHP

The standard VCHP cycle is shown in Figure 3.1. In this cycle, almost all processes involve changes in enthalpy in which case, by definition, heat and/or mechanical work (associated with pressure and volume changes) are being exchanged, neglecting changes in kinetic and potential energy of the fluid.

From points 1 to 2, the enthalpy of the vapour is increased through compression, and the specific work performed on the system is equal to the enthalpy variation:

$$w_c = h_2 - h_1 \tag{3.4}$$

Between 2 and 3, the fluid cools and condenses in a condenser, releasing heat into the HT reservoir at the condensation temperature:

$$q_{cond} = h_2 - h_3 \tag{3.5}$$

Between 3 and 4, the liquid is expanded into the two-phase region. If this happens in a throttling valve, the process is isenthalpic as heat exchanges can be neglected, and no work is performed on the surroundings. This process is highly irreversible, so it can never be isentropic.

$$h_3 = h_4 \tag{3.6}$$

Finally, the two-phase mixture receives energy in the evaporator and the fluid returns to a gas state, removing heat from the LT reservoir at the evaporation temperature:

$$q_{evap} = h_1 - h_4 \tag{3.7}$$

The COP of the heat pump in heating mode is given by the ratio between the heat released from the condenser and the energy consumed in compression. This value is generally greater than unity.

$$COP = \frac{q_{cond}}{w_c} \tag{3.8}$$

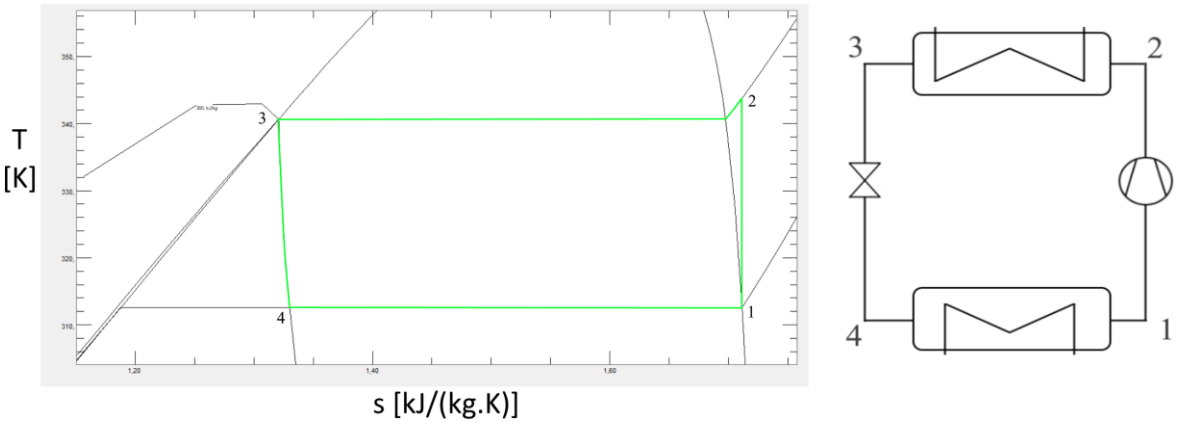

Figure 3.1. T-s diagram of a generic VCHP with isentropic compression (left), schematic representation of the simple VCHP (right) with matching state points; R-134a

In reality, compression may be non-isentropic and there may be superheating of the vapour at point 1, as well as subcooling of the liquid at point 3, in which case the cycle is as shown in Figure 3.2. When the compression process is non-isentropic, which is the case with all real compression processes, the specific entropy of the fluid increases from 1 to 2 – this translates into higher compression work for the non-isentropic process. The isentropic efficiency of a compressor can thus be defined as the ratio between the specific work of the compressor in the isentropic scenario and that of the real scenario:

$$\eta_{s,c} = \frac{w_{c,s}}{w_c} = \frac{(h_{2,s} - h_1)}{(h_2 - h_1)}, \tag{3.9}$$

Where $\eta_{s,c}$ is the compressor isentropic efficiency, w is the specific compression work, and h is the enthalpy of the working fluid at each point. The subscript s indicates an isentropic process.

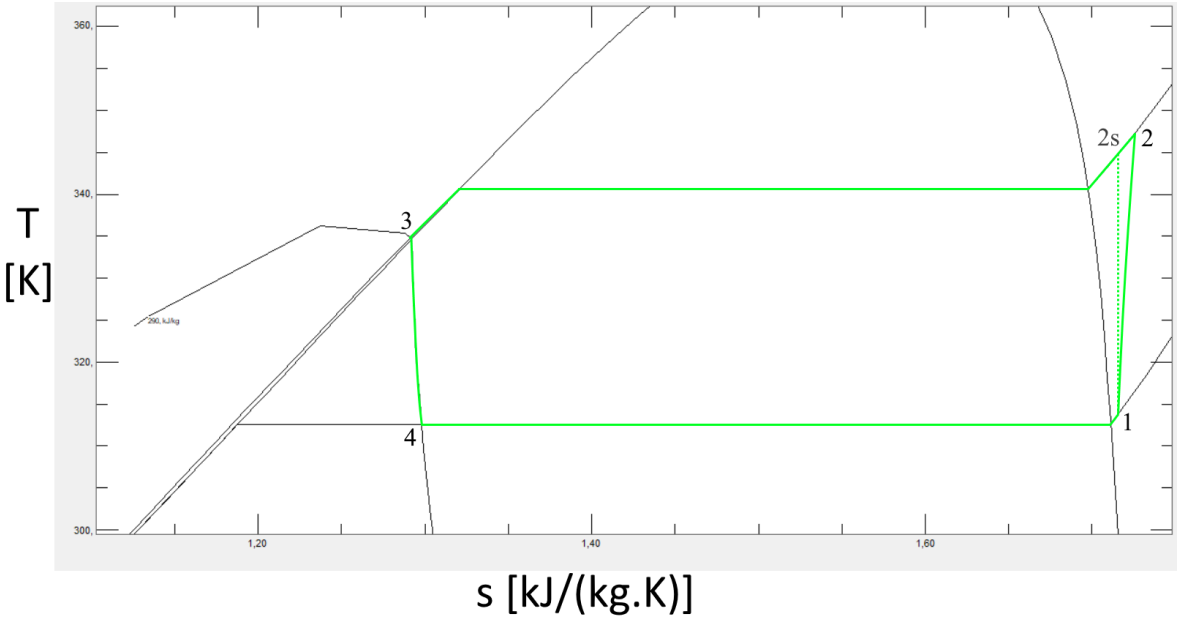

Figure 3.2. T-s diagram of a generic VCHP with non-isentropic compression, subcooling and superheating; R-134a

3.2.2. Simple ORC

In the Organic Rankine cycle – shown in Figure 3.3 – all processes involve enthalpy changes, as heat and/or mechanical work are exchanged at every step.

Between 1 and 2, the vapour is expanded, generating mechanical work – the enthalpy variation is equal to the specific work produced by expansion:

$$w_{exp} = h_1 - h_2 \tag{3.10}$$

From 2 to 3, the working fluid is condensed, rejecting heat to the LT reservoir:

$$q_{cond} = h_2 - h_3 \tag{3.11}$$

Subsequently, the liquid is pumped to the high pressure level. The enthalpy variation is equal to the specific work performed by the pump, however this value is very low as the entire process happens in the liquid phase.

$$w_{pump} = h_4 - h_3 \tag{3.12}$$

Finally, the pressurized liquid is heated and vaporized in the evaporator, drawing heat from the HT reservoir and returning to the state of point 1.

$$q_{evap} = h_1 - h_4 \tag{3.13}$$

The efficiency of the ORC is given by the ratio between the net energy output, and the heat input at the evaporator:

$$\eta = \frac{w_{exp} - w_{pump}}{q_{evap}} \tag{3.14}$$

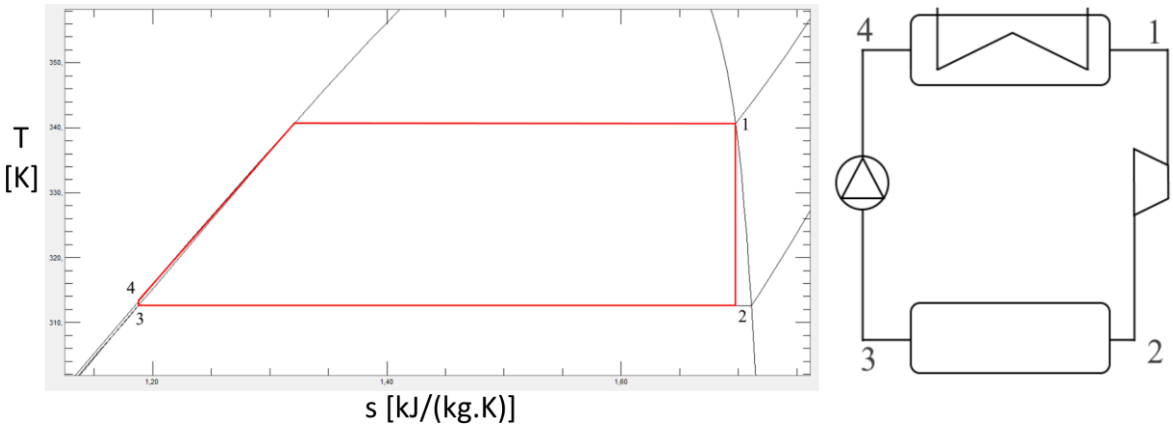

Figure 3.3. T-s diagram of a generic ORC with isentropic expansion and pumping (left), schematic representation of the simple ORC (right) with matching state points; R-134a

As with the vapour compression cycle, the real Rankine cycle involves irreversibilities, some of the most significant being the non-isentropic behaviour of the expander and the pump. The isentropic efficiencies of these machines are defined the same way as with the compressor – a ratio between an ideal and a non-ideal amount of work between two states:

$$\eta_{s,exp} = \frac{w_{exp}}{w_{exp,s}} = \frac{(h_1 - h_{2,s})}{(h_1 - h_{2,s})}, \tag{3.15}$$

$$\eta_{s,pump} = \frac{w_{pump,s}}{w_{pump}} = \frac{(h_{4,s} - h_3)}{(h_4 - h_3)}, \tag{3.16}$$

There may also be superheating of the vapour, to avoid two-phase expansion, or subcooling of the liquid to guarantee the absence of vapour in the pump. With non-isentropic processes and subcooling/superheating, the cycle takes the form shown in Figure 3.4.

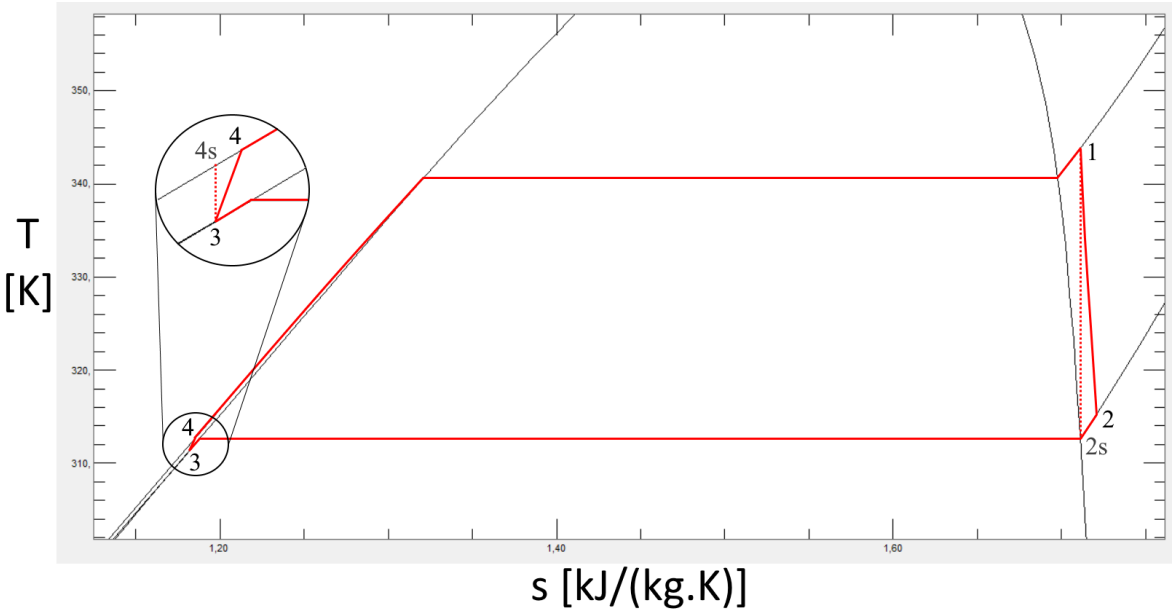

Figure 3.4. T-s diagram of a generic ORC with non-isentropic expansion and pumping, superheating and subcooling of the working fluid, detail view of the non-isentropic pumping process; R-134a

3.3. Storage Simulation and Iterative Cycle

The TES may use a Sensible Heat Material (SHM), or a Phase Change Material (PCM). PCMs are more energy dense and work well with isothermal processes, however they're often costlier than SHMs [5]. For each case the choice of storage material should be based on several technical, economic, and environmental criteria, a process which is largely outside the scope of this work.

Water was chosen as a SHM in the present case, as it presents a high specific heat capacity, low costs and no environmental concerns. To simulate this, a dynamic model was developed which considers the energy content in an insulated cylindrical tank at several points inside a specified time interval, applying an energy balance that takes into account charge power, discharge power, and losses to the environment.

Before the iterative process begins, various inputs are considered for a preliminary simulation of the VCHP and ORC. This determines reference values for mass flow and VCHP/ORC condenser and evaporator power, which are then used to design heat exchange areas for these components.

After this step, the thermal loss coefficient for the water tank is calculated, its value calculated by the inverse of the sum of a series of thermal resistances corresponding to the

thermal barriers that were considered – conduction through a layer of steel and a layer of insulation material, and a convective resistance on the outside of the tank.

$$U_{storage} = \left(R_{cond,steel} + R_{cond,insulation} + R_{conv}\right)^{-1} \quad [W \cdot m^{-2} \cdot K^{-1}] \tag{3.17}$$

Where the thermal resistances are given by:

$$\begin{cases} R_{cond} = \dfrac{t}{k} \\ R_{conv} = \dfrac{1}{h} \end{cases} \quad [m^2 \cdot K \cdot W^{-1}] \tag{3.18}$$

Where t is the thickness of the solid layer in metres, k its thermal conductivity in W/(m.K), and h is the convection coefficient in the units W/(m^2.K).

After these calculations, the cycle begins – each iteration starts by simulating the HP and ORC cycles dynamically, varying the condenser and evaporator temperatures according to the storage tank temperature, and until the heat exchange rate matches the thermal power associated with phase change.

The phase change (evaporation/condensation) power is calculated by the equation:

$$\dot{Q} = \dot{m} \cdot \Delta h \quad [W] \tag{3.19}$$

Where Δh is the enthalpy variation across the phase change. The rates of heat exchange are determined from the equation:

$$\dot{Q} = U \cdot A \cdot \Delta T \quad [W] \tag{3.20}$$

Where $\dot{Q}$ is the rate of heat transfer, U is a heat transfer coefficient, A is a heat transfer area, and ΔT is a temperature difference.

In the VCHP condenser and ORC evaporator, the temperature difference is established between the organic fluid and the thermal storage; in the VCHP evaporator it is between the organic fluid and the additional exergy source (if any exists), and in the ORC condenser it is between the organic fluid and the environment.

The heat exchange area A is previously determined for each component based on predicted working conditions, and the heat transfer coefficient U is modelled by an average value for phase change processes [21].

In standby mode, $\dot{Q}$ represents the rate of heat loss from the storage to the environment, U becomes $U_{storage}$, A is the surface area of the cylindrical reservoir, and ΔT is the temperature difference between the water and the outside air at each iteration.

After the thermodynamic cycles have converged, the energy balance is calculated:

$$E_t = E_{t-1} - \left(\dot{Q}_{loss} \times \Delta t\right) + \left(\dot{Q}_{ch} \times \Delta t\right) - \left(\dot{Q}_{dch} \times \Delta t\right) \quad [J] \tag{3.21}$$

Where t is the current time step, E is the thermal energy content of the mass of water, Δt is the length of the time step, and $\dot{Q}_{loss}$, $\dot{Q}_{ch}$ and $\dot{Q}_{dch}$ are the heat transfer rates calculated earlier in the iteration, representing loss to the environment, charge, and discharge respectively.

The new energy value is then used to update the temperature of the water, which is considered to stay in the liqid state, using the equation:

$$T_t = \frac{E_t}{m \cdot c_p} \quad [K] \tag{3.22}$$

Values of interest (temperature, heat transfer ratios, etc.) are stored, and the next cycle begins with the new temperature value. The calculation ends after a specified time interval, or when a stopping criterion is reached.

This algorithm is schematized in Figure 3.5. To summarize, the cycle begins by considering the first inputs provided by the user, then it proceeds to preliminary calculations of the cycles, from which it moves to the next step where it designs the heat exchangers and calculates the physical properties of the storage tank. After this, the iterative cycle begins, inside of which the temperatures of the various points in the thermodynamic cycles, as well as the storage temperature, are constantly updated. The cycle stops when a stopping criterion (for example, a maximum/minimum temperature) is reached, or when it reaches the end of the specified time interval, and then final values are logged and plotted depending on the user's needs.

One way of utilizing this algorithm is to adjust the input parameters based on the output of the cycle, running the program several times until the desired results are achieved – this was done in this work, and the process is explained in Chapter 4.

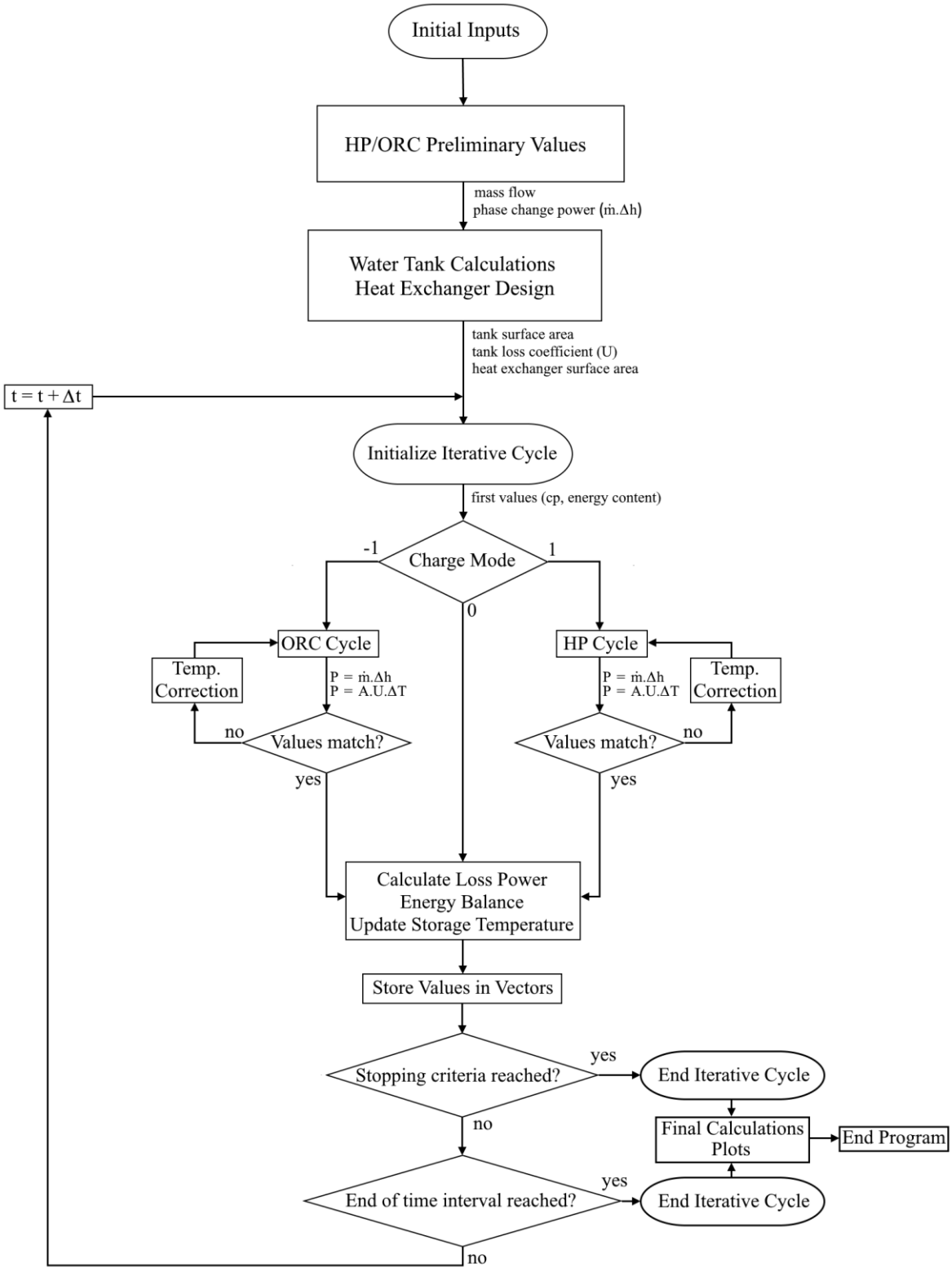

Figure 3.5. Flowchart representation of the algorithm used in the MATLAB script

4. CASE STUDY

Using the model developed in Chapter 3, the case of a solar PV power plant will be analysed. Excess power from the PV array is to be stored as thermal exergy in the water tank and used at night when the solar panels cannot provide any energy.

As a means of thermal integration, a solar thermal system is used in conjunction with a secondary hot water tank to boost the temperature of the VCHP evaporator to 70°C. The VCHP compressor receives excess electric energy from the solar PV panels and uses it to upgrade the heat from the evaporator to the required temperature at the condenser.

The hot water from the main water tank is then used as a heat source for the ORC, which produces electric energy in the expander as it discharges this heat to the environment.

Figure 4.1 shows the layout of the proposed system.

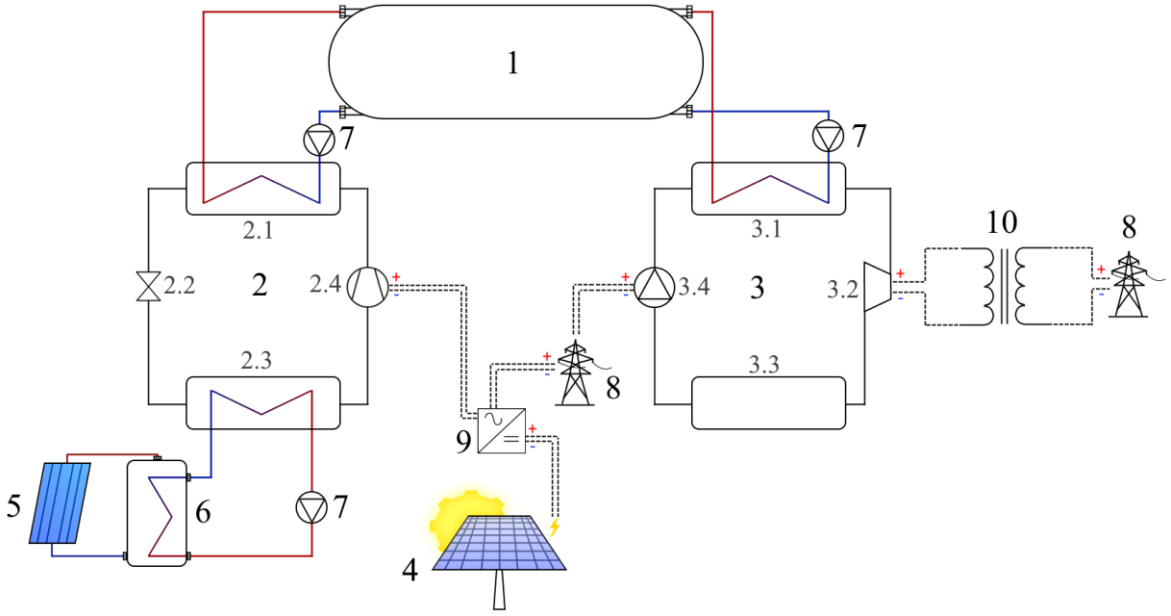

Figure 4.1. Schematic representation of the proposed system (**1**-Water Tank; **2**-Heat Pump; **2.1**-HP Condenser; **2.2**-HP throttling valve; **2.3**-HP Evaporator; **2.4**-HP Compressor; **3**-ORC; **3.1**-ORC Evaporator; **3.2**-ORC Expander; **3.3**-ORC Condenser; **3.4**-ORC Pump; **4**-PV Array; **5**-Solar thermal panel; **6**-Hot water tank; **7**-Pump; **8**-Power grid; **9**-DC/AC Converter; **10**-AC Transformer)

4.1. Validation

With the battery model revealed in section 3.1 and its proposed application in mind, a first charge/standby/discharge cycle was performed to compare with other studies and obtain initial results and a primary validation, using the values in Table 4.1.

For this first run, a full charge was simulated, followed by 4 hours of standby, and finally a complete discharge of the storage, returning to the initial temperature.

Table 4.1. Initial Storage Simulation Parameters

Parameter	Value	Unit
(Water Tank)		
Volume	5	m^3
Aspect Ratio (Length/Diameter)	2	-
Pressure (Absolute)	101.325	kPa
Steel Thickness	0.01	m
Steel Termal Conductivity	50	W/(m.K)
Insulation Thickness	0.05	m
Insulation Thermal Conductivity	0.05	W/(m.K)
(VCHP)		
Condenser Temperature (design value)	100	°C
Evaporator Temperature (design value)	60	°C
Compressor Isentropic Efficiency	0.7	-
Compressor Power (design value)	1000	W
Subcooling	0	°C
Superheating	0	°C
Condenser Heat Transfer Coefficient (U)	1000	$W/(m^2.K)$
(ORC)		
Condenser Temperature (design value)	35	°C
Evaporator Temperature (design value)	60	°C
Expander Isentropic Efficiency	0.7	-
Expander Power (design value)	1000	W
Pump Isentropic Efficiency	0.8	-
Subcooling	0	°C
Superheating	0	°C
Evaporator Heat Transfer Coefficient (U)	1000	$W/(m^2.K)$
(Other)		
Ambient Temperature	25	°C
Time Step	30	s
Ambient convection coefficient	10	$W/(m^2.K)$
Electric motor/generator average efficiency	0.95	-
Heat exchangers pinch point (design value)	10	°C

The charge phase brought the storage up to a temperature of 90°C in about 17 hours and 46 minutes, with 123.6 kWh of thermal energy variation in the water. With a total electrical consumption of 13.54 kWh, this leads to a global COP of 9.13, factoring in thermal losses to the environment during the charge; if the losses are not considered, the COP is 10.41 – the first value considers the performance of the VCHP and the storage, whereas the second only considers the performance of the VCHP.

The exact values change throughout the charge, as shown in Figure 4.2, with an increase in compressor work and a decrease in condenser thermal power release as the temperature and pressure in the condenser increase, leading to a decrease in the COP.

It can be observed that the VCHP has taken a relatively long time to charge the storage – the charging time mostly depends on the ratio between the total storage heat capacity and the charge power of the heat pump, which has the units [°C/s].

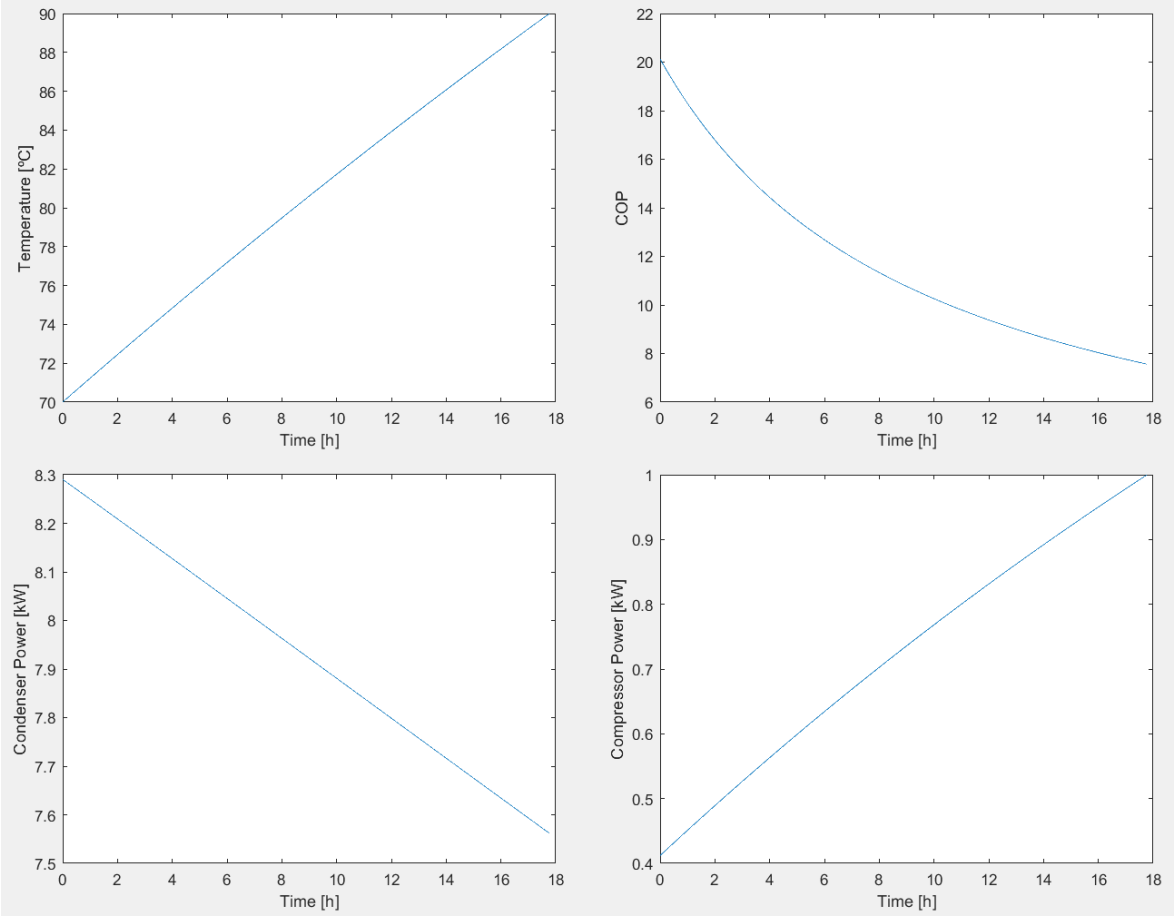

Figure 4.2. Evolution of key parameters in the charge phase

During the standby phase, the temperature of the storage tank was brought down slightly due to losses to the environment, with a reduction from 90°C to 89.28°C. This

decrease of 0.72°C corresponds to a loss of 4.53 kWh of thermal energy. Figure 4.3 shows the evolution of the temperature and the thermal loss power from the water tank over the 4 hour period.

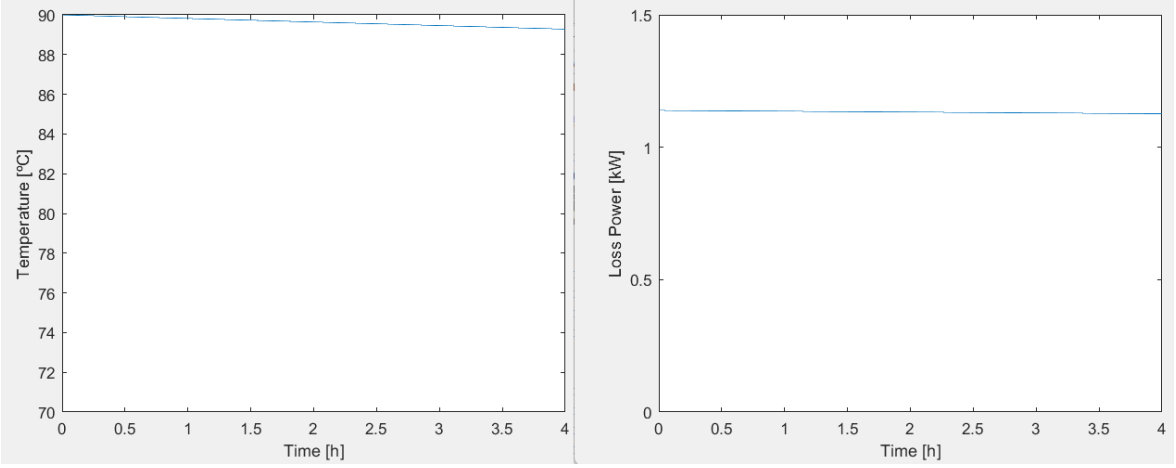

Figure 4.3. Evolution of key parameters in the standby phase

Finally, the discharge phase brought the storage temperature back down to 70°C in about 10 hours and 27 minutes, with a thermal energy reduction of 119.06 kWh, and a net electrical generation of 8.08 kWh, leading to a global Rankine efficiency of 6.8%; factoring out losses to the environment, the global efficiency of the ORC is 7.4%.

With the decrease in evaporator temperature and pressure comes a decrease in evaporator thermal power consumption as well as expander power generation and pump power consumption, with an overall decrease in efficiency.

Roundtrip efficiency is often estimated as the product of the COP with the Rankine efficiency, however this becomes inaccurate when thermal losses from the storage are considered. The use of a dynamic model allows the calculation of a precise value – in this first case, an ε_{rt} of 59.7% was obtained – a value consistent with those obtained in previous studies, and a satisfactory value for a a non-optimized situation.

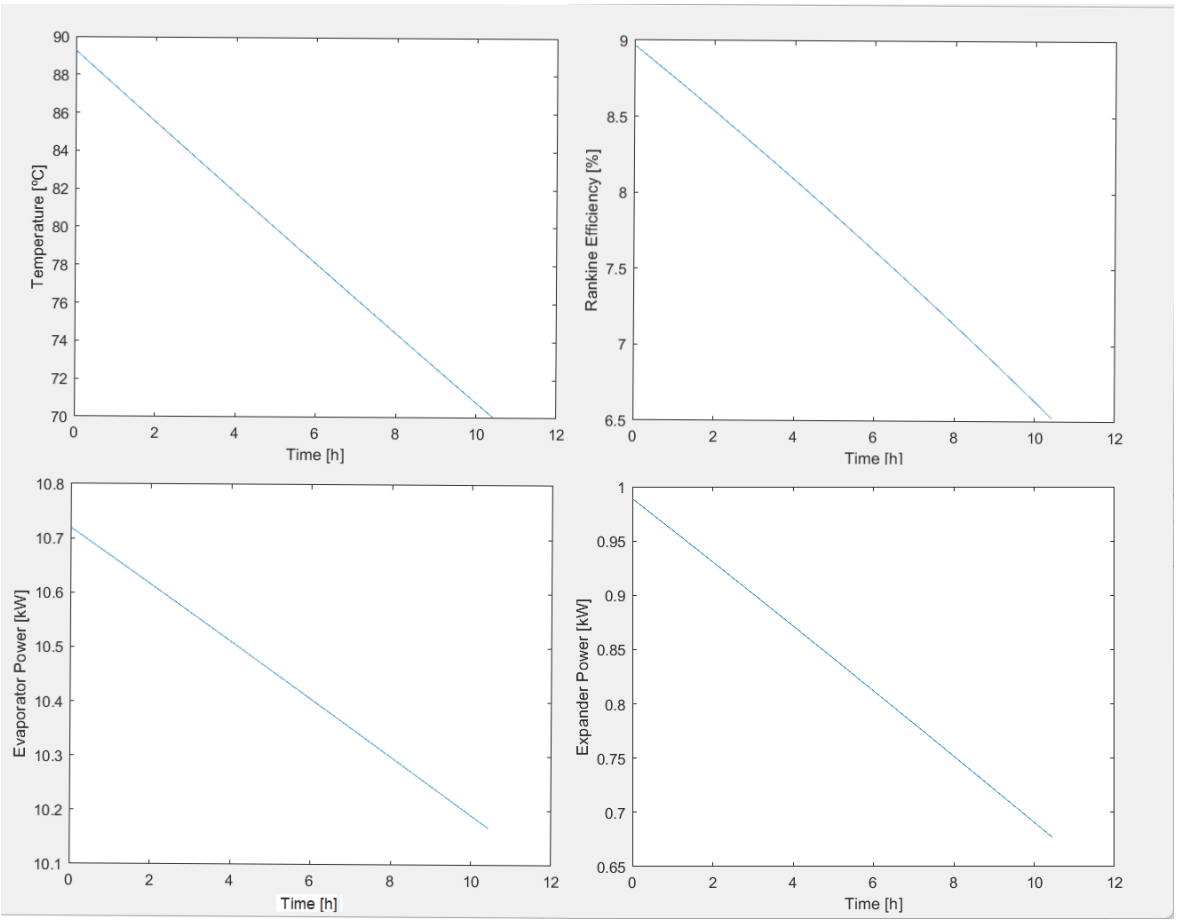

Figure 4.4. Evolution of key parameters in the discharge phase

4.2. Optimization Method

With an initial validation established, a more specific case can be studied and optimized.

The main driving parameters are expander power, discharge time and charge time. These first two parameters determine an energy requirement, thus allowing the design of an adequate storage size. The heat pump can then be designed for a power which allows a full charge in 8 hours – roughly the time during which solar energy is available for the PV array.

In terms of optimization, the main objectives are the storage size/temperature variation and heat exchanger surface areas/pinch points, the pinch point being the minimum temperature difference between the two fluids in a heat exchanger. The optimization of these parameter couples involves a balance between cost and performance, as the best performance results from the largest surface areas and storage volumes, as these reduce the temperature differences, but they also lead to greater costs.

To evaluate the effect of these parameters, a full discharge and a full charge were simulated for five nominal pinch point values (10K, 8K, 6K, 4K, 2K), and five storage temperature spreads at each pinch point (70°C – 75°C, 70°C – 80°C, 70°C – 85°C, 70°C – 90°C and 70°C – 95°C), resulting in a total of 25 charge simulations and 25 discharge simulations.

For each case, the storage size was optimized for a 4-hour discharge with a nominal expander power of 20kW, and then a nominal compressor power was chosen to allow a full charge of the storage in 8 hours – these reference powers correspond to the maximum values that will be encountered throughout the simulation.

In terms of costs, the correlations in Table 4.2 were used to provide a rough estimate for capital costs in order to make the cost/performance optimization possible. The total cost of the system is given by the sum of the costs for each component.

Table 4.2. Cost Correlations for components used in the Carnot Battery

Component	Cost Correlation [€]	Unit of Independent Variable	Source
Storage Tank	$2000 + (625 \times Vol._{storage})$	m^3	-
Heat Exchangers	$150 \times Area$	m^2	[22]
ORC Expander	$1.5 \times (225 + (17000 \times \dot{V}_{in}))$	m^3/s	Adapted from [22]
ORC Pump	$900 \times (\dot{W}_{pump}/300)$	W	[22]
VCHP Compressor	$225 + (17000 \times \dot{V}_{in})$	m^3/s	Adapted from [22]
Control Electronics	4000	-	-

4.3. Results and Discussion

Figure 4.5 shows the values that were obtained for roundtrip efficiency at each pinch point, and for all the storage spreads that were tested – the higher efficiency values correspond to lower storage temperature spreads, and vice-versa.

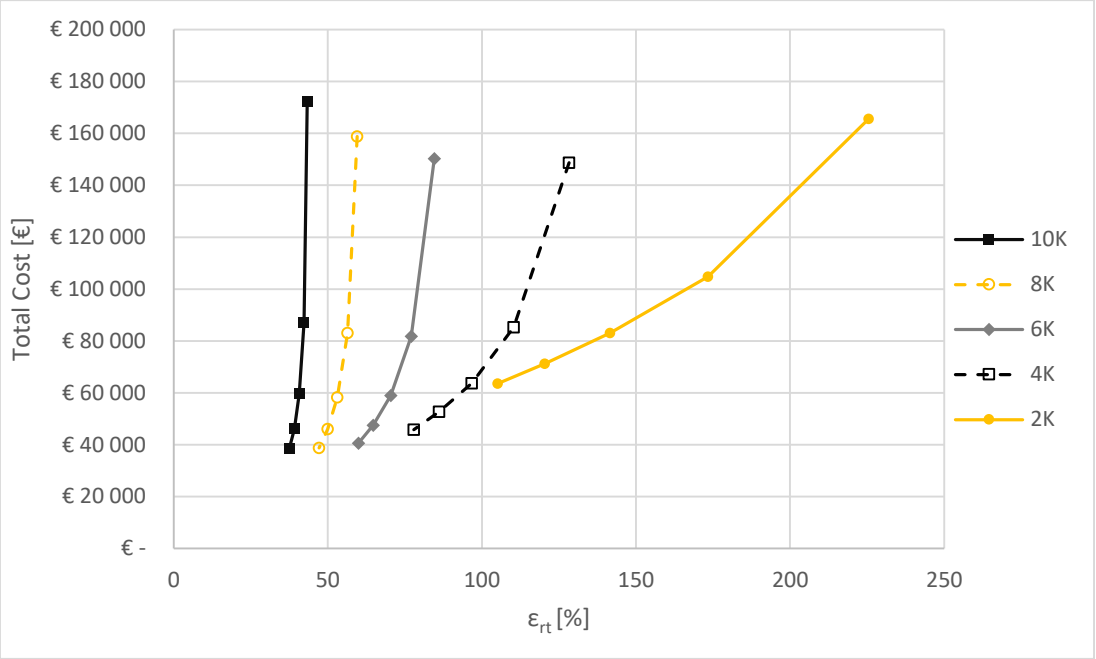

Figure 4.5. Roundtrip efficiency vs. cost for various pinch points

As expected, lower pinch points lead to higher roundtrip efficiency for any storage spread, as this minimizes the temperature gradient of the VCHP and maximizes it for the ORC. A lower storage spread also improves efficiency, as it greatly increases the COP, with only a small decrease in ORC efficiency.

In terms of costs, while the lower pinch points and lower storage spreads lead to higher values (larger heat exchangers and storage tank), the effect of the storage spread seems far greater than that of the pinch point, so the best cost/efficiency ratios are mostly found with the lower pinch points and higher storage spreads – the highest value was obtained for the 10K pinch point and 70°C – 75°C storage spread, at 3979.70 [€/% roundtrip efficiency], with an ε_{rt} of 43.32%. By contrast, the best cost/efficiency ratio was obtained for the 2K pinch point and 70°C – 85°C storage spread, with a value of 586.73 [€/% roundtrip efficiency], and an ε_{rt} of 141.54%.

For the 2K pinch point, all storage spreads above 70°C – 75°C return cost/efficiency values below 605 [€/% roundtrip efficiency], with roundtrip efficiencies between 173-105%. At this pinch point, the highest performance is reached with a 70°C – 75°C spread, at a cost/efficiency of 734.37 [€/% roundtrip efficiency], but with an ε_{rt} of 225.54%. In all cases for the 2K pinch point, the system becomes a hybrid between energy storage and a solar thermal power plant, as the efficiency exceeds 100%.

Figure 4.6 shows how the storage spread (70 – maximum temperature) and pinch point influence the cost/efficiency ratio. It can again be seen that most points along the 2K line are close to the optimal value.

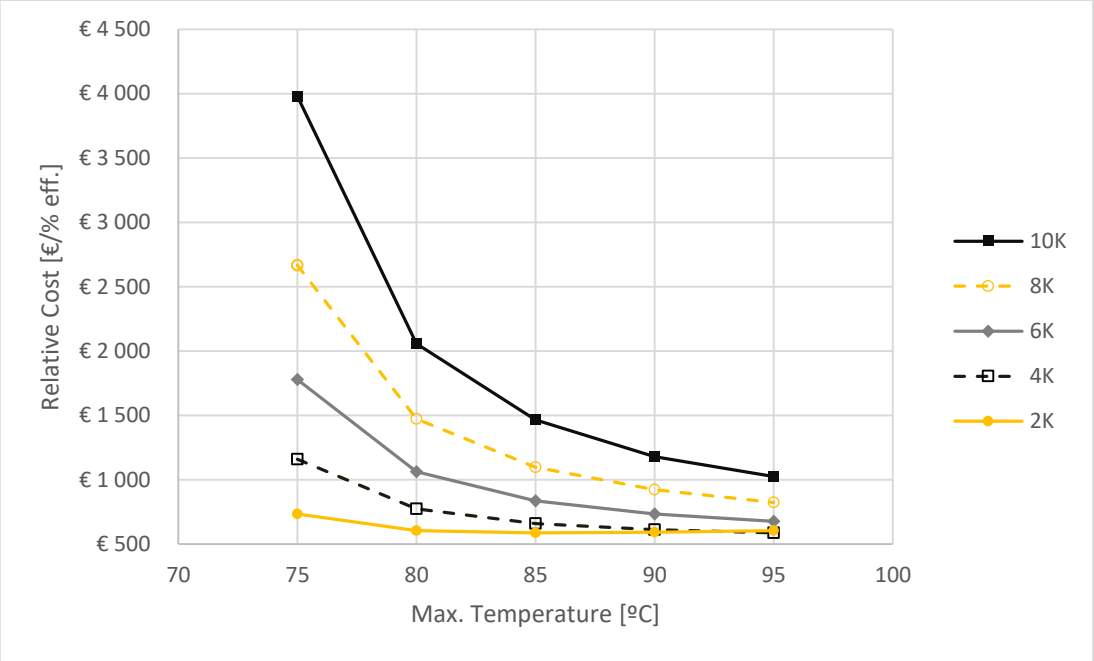

Figure 4.6. Maximum storage temperature vs. relative cost for various pinch points

In Figure 4.7 and Figure 4.10 the cost of the storage tank and the heat exchangers, respectively, are shown for each pinch point/storage spread configuration.

The storage spread has the largest influence on tank cost, as it directly influences the size of the storage tank; the pinch point also has a small effect, as higher efficiencies demand less energy in the storage for a given output.

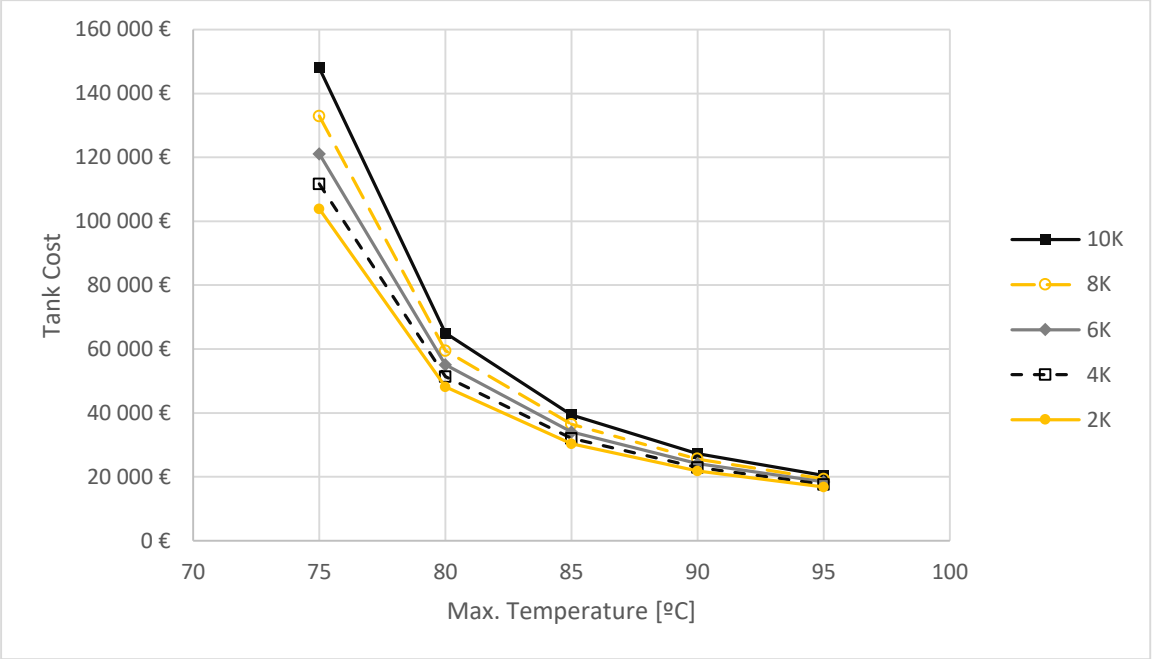

Figure 4.7. Maximum storage temperature vs. storage tank costs for various pinch points

For the heat exchanger costs, the pinch point has the largest influence as it determines the required heat transfer area – lower pinch points requite larger transfer areas, and vice-versa, to maintain a similar heat exchange rate. The storage spread also has an effect on heat exchanger size, as the reference machines exchange less power in their design conditions for higher spreads.

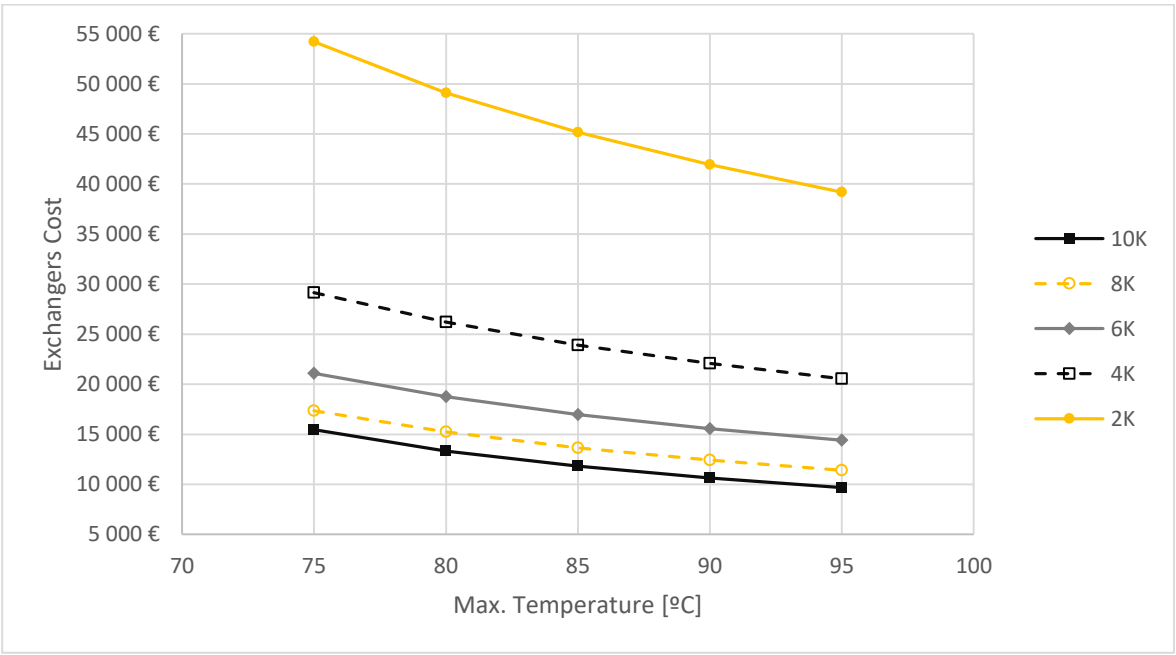

Figure 4.8. Maximum storage temperature vs. cost of heat exchangers for various pinch points

In Figure 4.9 and Figure 4.10 the evolution of the ORC and VCHP mass flow, respectively, is shown.

While the VCHP has generally lower mass flow values (mostly a result of low compressor power demand), the trend in both cycles is a decrease in mass flow with an increase in storage spread and a decrease in pinch point. This is due to the increase in specific compressor/expander work that accompanies a larger temperature gradient – since the mass flow is calculated as the ratio between compressor/expander power and specific work, an increase in specific work will always cause a decrease in mass flow if the machine power is unchanged. In the case of the VCHP, the compressor power actually decreases with the lower pinch points, which further reduces the mass flow.

While the cost of piping was not included in the present calculations, the lower mass flow rates would certainly lead to smaller and cheaper pipes, which would make the systems with lower pinch points and higher storage spreads even more economically attractive.

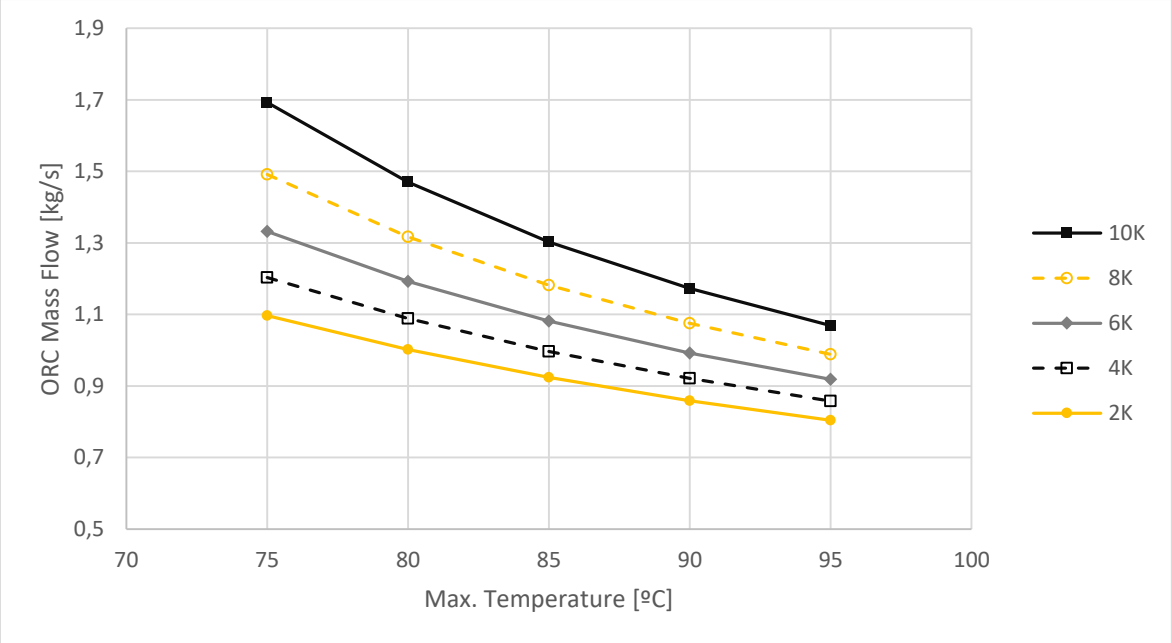

Figure 4.9. Maximum storage temperature vs. ORC mass flow for various pinch points

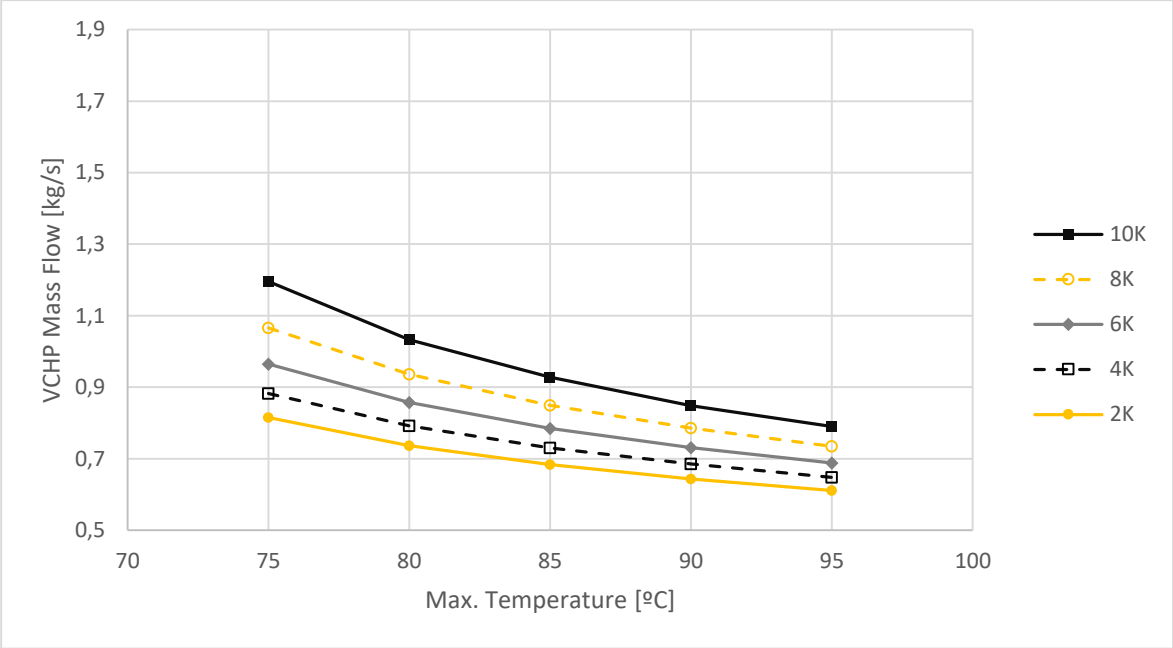

Figure 4.10. Maximum storage temperature vs. VCHP mass flow for various pinch points

Figure 4.11, Figure 4.12 and Figure 4.13 show the costs of the ORC expander, ORC pump and VCHP compressor, respectively, for each pinch point/storage spread.

The expander cost decreases with increasing spread and decreasing pinch point, as the decrease in mass flow typically commands a lower volumetric flow rate. The 2K pinch point leads to the lowest expander costs, as the mass flow is lowest for all storage spreads in this situation.

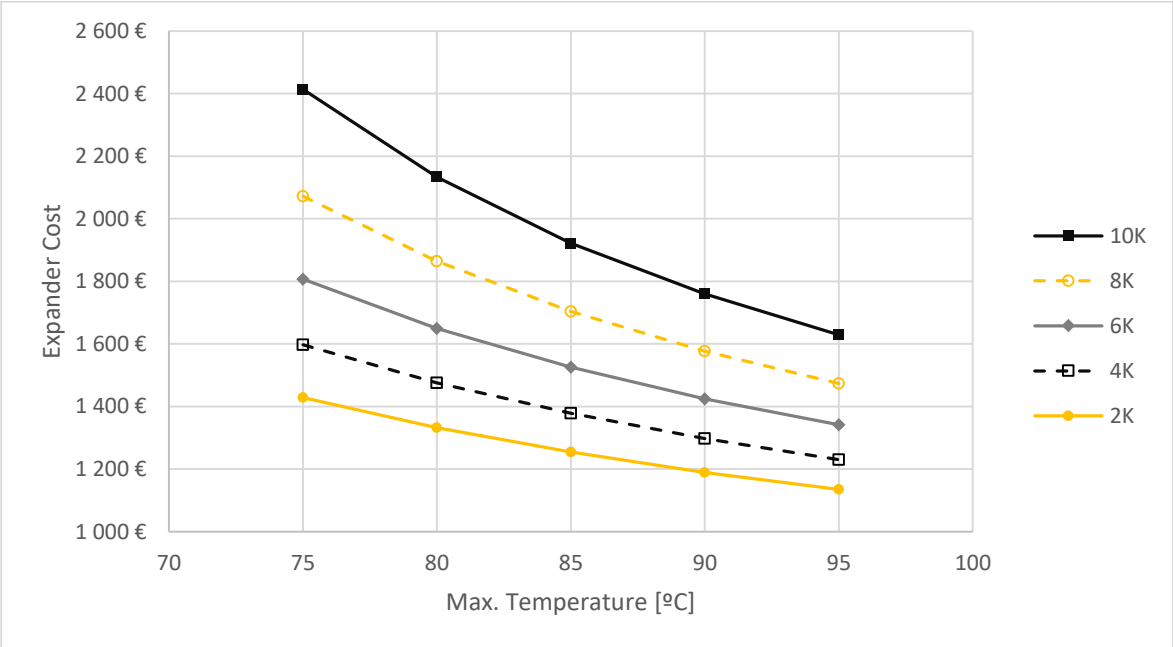

Figure 4.11. Maximum storage temperature vs. ORC expander cost for various pinch points

The pump cost grows mostly with an increase in storage spread, as the larger temperature (and pressure) gradient requires more pumping work. The effect of the pinch point is very low, however the 2K pinch point will always result in the lowest pump cost.

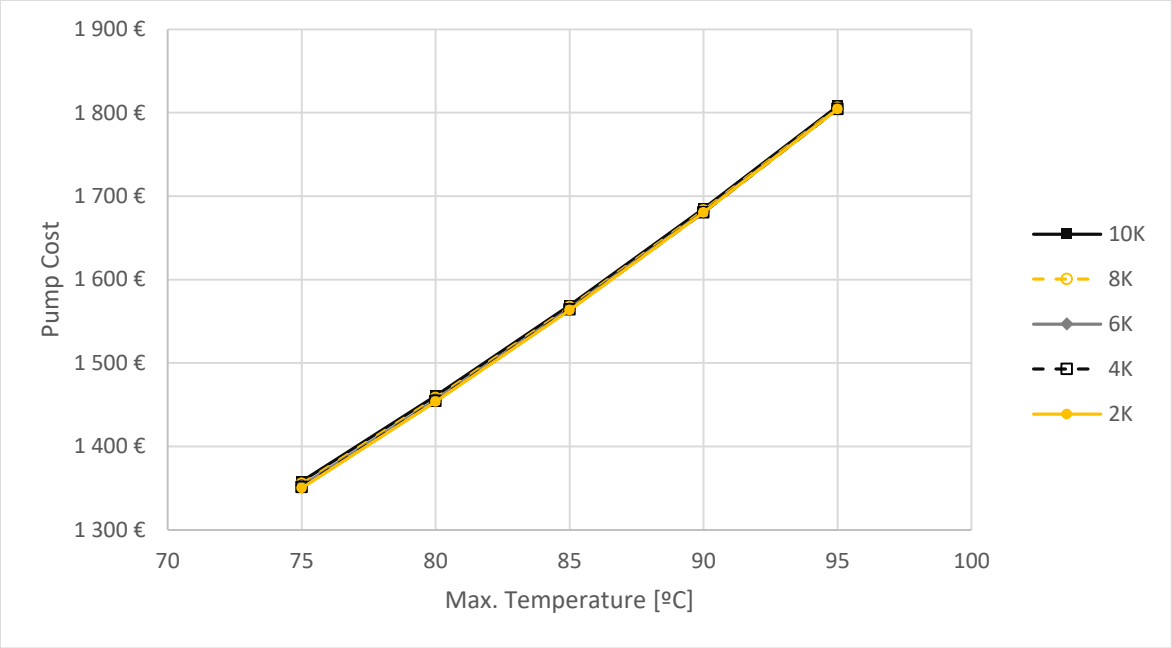

Figure 4.12. Maximum storage temperature vs. ORC pump cost for various pinch points

The effect is similar for the VCHP compressor as for the ORC expander – lower pinch points and higher spreads result in decreased mass flow rates, which results in lower volume flow rates at the compressor inlet. Additionally, the improved COP at lower pinch points means the heat pump requires less compressor power for the same heating effect, which further decreases mass flow, volume flow, and subsequently cost.

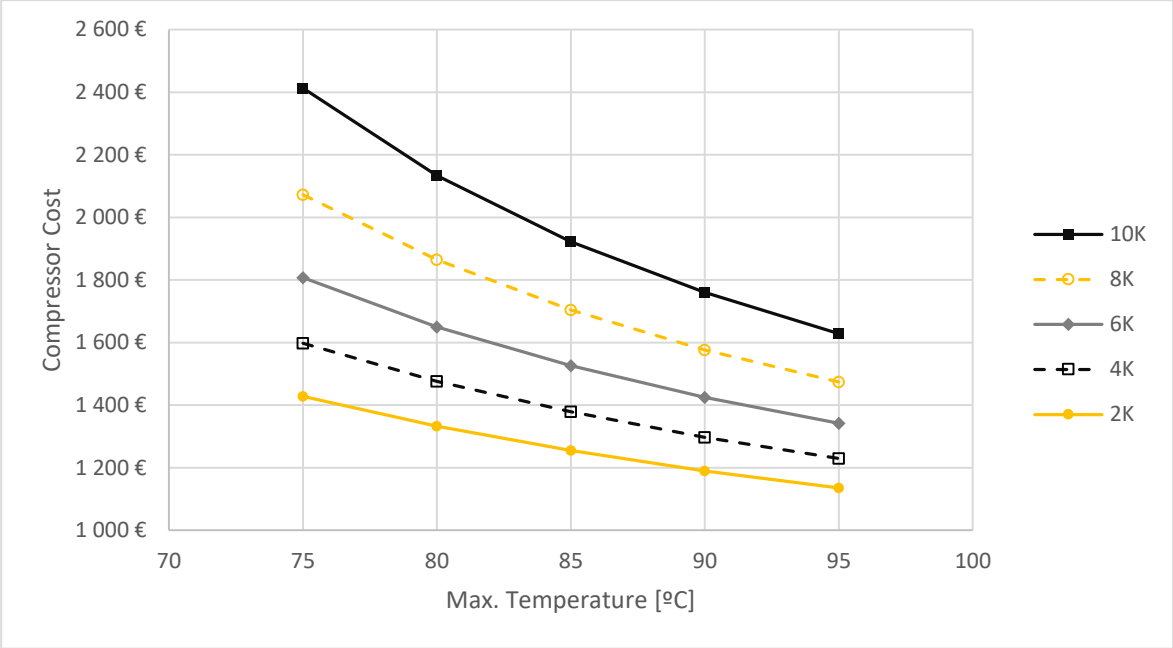

Figure 4.13. Maximum storage temperature vs. VCHP compressor cost for various pinch points

Finally, payback time was analysed for the various configurations, as shown in Figure 4.14.

The daily profit was calculated as the total electric energy of the discharge phase multiplied by a price of 0.20 €/kWh – a value assumed based on the costs of a few energy providers available in Portugal (EDP, Galp, Goldenergy) [23]–[25] as well as reference values from the Energy Services Regulatory Authority (ERSE) [26], for a contracted electric power up to 20.7 kVA.

Furthermore, the system was assumed to generate this daily profit for 12 months of the year; in reality the performance would generally worsen in the winter months leading to lower profits. Even with enough solar thermal panels to offset unfavourable climate conditions, this fact could potentially affect the payback period in a real situation.

For all storage configurations, the shortest payback times are generally achieved with the 4K, 6K and 8K pinch points, and the shortest payback time between all the simulations is obtained with the 70°C – 95°C spread: approximately 9 years and 2 months. For a payback time of 4 years or lower, the average price of electricity would need to be at least 0.46 €/kWh.

Every configuration presents a payback time between 9 and 35 years.

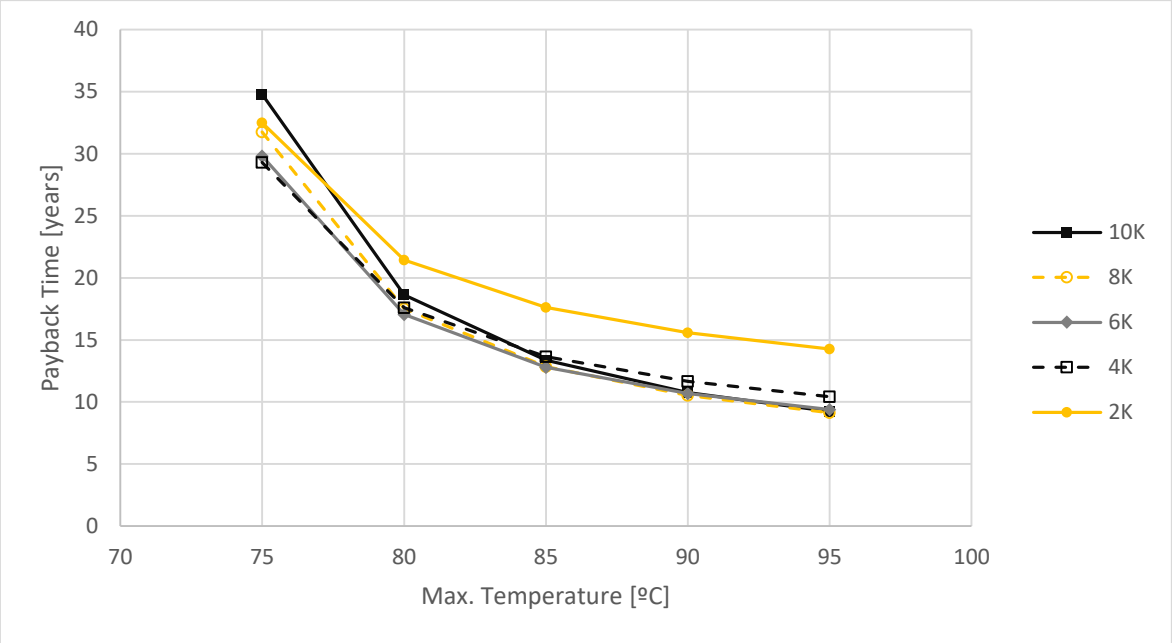

Figure 4.14. Maximum storage temperature vs. payback time for various pinch points

It can be concluded that a select few configurations optimize one parameter or another – the lowest pinch point (2K) and lowest storage spread (70°C – 75°C) optimize performance, the highest pinch point (10K) and the highest spread (70°C – 95°C) optimize costs, the 2K pinch point and 70°C – 85°C spread optimize the cost/performance ratio, and the 8K pinch point and 70°C – 95°C spread optimize the payback period. In this case, all of these solutions are ideal in one form or another – these configurations belong on the so-called Pareto Front (Figure 4.15), the set of all Pareto-optimal solutions. In other words, by moving between the points on this line it is impossible to improve any criterion without deteriorating another. This means that any point on this line represents a valid choice, and the selection should depend on the most relevant priority, or a balance of relevant priorities for a given implementation.

For example, from a technological perspective, the best choice is the one with the highest efficiency. In terms of budget alone, the best choice has the lowest cost. For an efficient capital investment, one would select the machine with the best cost/performance ratio, and to minimize the risk of investment the machine with the lowest payback time should be chosen.

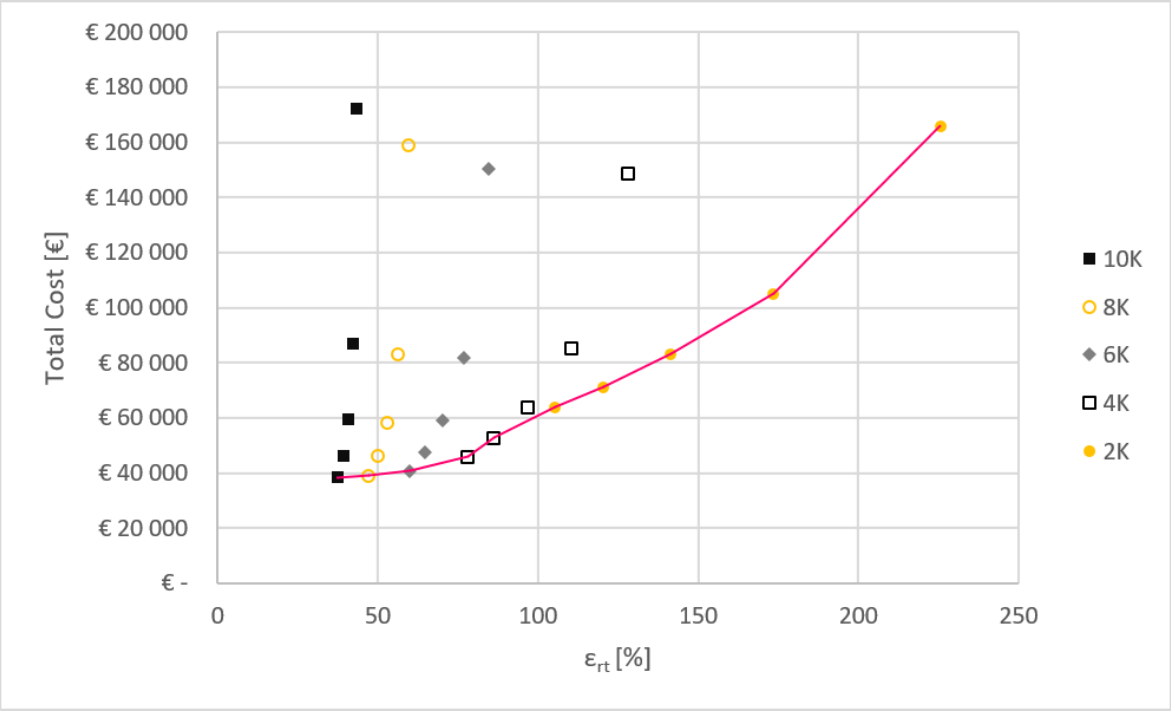

Figure 4.15. Pareto Front for the tested configurations

4.4. Modified Cycles

To improve the performance of the cycles, multi-stage compression can be used for the VCHP and a regenerator can be installed in the ORC, among other modifications. These variants of the basic cycles were considered for the study, however the results from an initial analysis were not particularly promising – while the regenerative ORC delivered higher efficiencies, the multi-stage VCHP actually presents a lower heating COP than the standard cycle. In light of these results, the simple cycles were used; maintaining the simple cycles also allowed a better focus on the simulation algorithm as a whole.

5. CONCLUSIONS AND PERSPECTIVES

In this work, the motivation and state-of-the-art were explored for energy storage solutions, and a case was made for the Carnot Battery as a suitable technology to replace current systems with relatively low Power/Capacity ratios, and a storage duration in the range of a few hours.

Following this, a MATLAB script was developed which is capable of simulating the performance of a Carnot Battery composed of simple Vapour Compression Heat Pump and Organic Rankine Cycles in dynamic charge/discharge conditions, as well as the thermal behaviour of a sensible storage in a standby situation.

Despite the limited scope of the present study, the flexibility the developed model should allow its use in diverse situations with little to no modification, including off-design performance, thermal storage material selection, analysis of different thermal integration strategies, as well as more detailed techno-economic studies.

In the present work, the model was used to study several configurations, taking into account the most critical parameters of the system, in an effort to discover an optimized arrangement; in the end, the optimal configuration depends on a balance of priorities – if performance is the only criterion, the lowest pinch point (2K) and lowest storage spread (70°C – 75°C) should be selected despite the high costs; to minimize costs alone, one would select the highest pinch point (10K) and the highest spread (70°C – 95°C) in spite of the low efficiency, and for the best cost/performance ratio, the optimal choice would lie in between these two, with a 2K pinch point and a 70°C – 85°C spread. Additionally, for a minimized payback period the choice would be the 8K pinch point and a 70°C – 95°C spread.

It was concluded that these four points belong on the Pareto front, in which all points represent either the optimization of one parameter, or a compromise between multiple parameters, and conclusions were drawn as to the applicability of each configuration.

Looking forward, various improvements can be made to studies of this nature. Within the context of the proposed case study, the solar thermal system could be designed based on the global energy requirement of the VCHP evaporator, including the selection of solar thermal panels, piping, pumping system, and the secondary hot water tank. Another possibility would be a better cost estimation for a selected configuration, using market values

for real components in place of cost correlations, which would lead to more accurate estimates of cost and payback period. Different HP and HE archicectures could be studied, including modifications to the VCHP and ORC such as regenerative cycles and cascading systems, and a detailed selection of working fluids could be carried out for a given case.

In a more general perspective, transient models could be useful in addressing research gaps that can be identified in the current literature, such as dynamic and off-design performance of Carnot Battery systems as well as detailed technical and economical studies [5]. The degree of flexibility and physical accuracy provided by dynamic models can be helpful in closing such research gaps and bringing the technology to the market, alongside the use of prototypes for experimental validation.

REFERENCES

[1] A. B. Gallo, J. R. Simões-Moreira, H. K. M. Costa, M. M. Santos, and E. Moutinho dos Santos, "Energy storage in the energy transition context: A technology review," *Renewable and Sustainable Energy Reviews*, vol. 65. 2016. doi: 10.1016/j.rser.2016.07.028.

[2] S. I. Inage, "The role of large-scale energy storage under high shares of renewable energy," *Wiley Interdiscip. Rev. Energy Environ.*, vol. 4, no. 1, pp. 115–132, 2015, doi: 10.1002/wene.114.

[3] M. Jafari, A. Botterud, and A. Sakti, "Decarbonizing power systems: A critical review of the role of energy storage," *Renew. Sustain. Energy Rev.*, vol. 158, p. 112077, Apr. 2022, doi: 10.1016/J.RSER.2022.112077.

[4] M. M. Rahman, A. O. Oni, E. Gemechu, and A. Kumar, "Assessment of energy storage technologies: A review," *Energy Conversion and Management*, vol. 223. 2020. doi: 10.1016/j.enconman.2020.113295.

[5] O. Dumont, G. F. Frate, A. Pillai, S. Lecompte, M. De paepe, and V. Lemort, "Carnot battery technology: A state-of-the-art review," *J. Energy Storage*, vol. 32, no. July, 2020, doi: 10.1016/j.est.2020.101756.

[6] G. F. Frate, L. Ferrari, and U. Desideri, "Rankine carnot batteries with the integration of thermal energy sources: A review," *Energies*, vol. 13, no. 18, 2020, doi: 10.3390/en13184766.

[7] https://www.andritz.com/hydro-en/hydronews/hn32/11-pumped-storage (accessed Mar. 29, 2022).

[8] http://power-thru.com/ (accessed Mar. 29, 2022).

[9] https://en.wikipedia.org/wiki/Flow_battery (accessed Mar. 29, 2022).

[10] https://en.wikipedia.org/wiki/Sodium–sulfur_battery (accessed Mar. 29, 2022).

[11] https://pt.mouser.com/new/eaton/powerstor-eatonxl60-supercapacitors/ (accessed Mar. 29, 2022).

[12] https://www.researchgate.net/figure/Super-magnetic-energy-storage-SMES-system-design-66_fig2_329768714 (accessed Mar. 29, 2022).

[13] D. Enescu, G. Chicco, R. Porumb, and G. Seritan, "Thermal energy storage for grid applications: Current status and emerging trends," *Energies*, vol. 13, no. 2. 2020. doi: 10.3390/en13020340.

[14] A. A. Kebede, T. Kalogiannis, J. Van Mierlo, and M. Berecibar, "A comprehensive review of stationary energy storage devices for large scale renewable energy sources grid integration," *Renew. Sustain. Energy Rev.*, vol. 159, p. 112213, 2022, doi: 10.1016/j.rser.2022.112213.

[15] M. Weitzer, D. Müller, D. Steger, A. Charalampidis, S. Karellas, and J. Karl, "Organic flash cycles in Rankine-based Carnot batteries with large storage temperature spreads," *Energy Conversion and Management*, vol. 255. 2022. doi: 10.1016/j.enconman.2022.115323.

[16] O. Dumont and V. Lemort, "Mapping of performance of pumped thermal energy storage (Carnot battery) using waste heat recovery," *Energy*, vol. 211, p. 118963, 2020, doi: 10.1016/j.energy.2020.118963.

[17] W. D. Steinmann, D. Bauer, H. Jockenhöfer, and M. Johnson, "Pumped thermal

energy storage (PTES) as smart sector-coupling technology for heat and electricity," *Energy*, vol. 183, pp. 185–190, 2019, doi: 10.1016/j.energy.2019.06.058.
[18] B. Eppinger, D. Steger, C. Regensburger, J. Karl, E. Schlücker, and S. Will, "Carnot battery: Simulation and design of a reversible heat pump-organic Rankine cycle pilot plant," *Appl. Energy*, vol. 288, no. November 2020, p. 116650, 2021, doi: 10.1016/j.apenergy.2021.116650.
[19] S. Staub *et al.*, "Reversible heat pump-organic rankine cycle systems for the storage of renewable electricity," *Energies*, vol. 11, no. 6, 2018, doi: 10.3390/en11061352.
[20] D. Steger, C. Regensburger, B. Eppinger, S. Will, J. Karl, and E. Schlücker, "Design aspects of a reversible heat pump - Organic rankine cycle pilot plant for energy storage," *Energy*, vol. 208, p. 118216, 2020, doi: 10.1016/j.energy.2020.118216.
[21] https://www.engineersedge.com/thermodynamics/overall_heat_transfer-table.htm (accessed Jul. 01, 2022).
[22] M. D. A. Dos Santos, "Modular architecture of steady-state simulation of Rankine based micro combined heat and power systems," no. October, 2020.
[23] https://www.edp.pt/particulares/energia/tarifarios/ (accessed Jul. 09, 2022).
[24] https://casa.galp.pt/ajuda/precos-faturacao-e-pagamentos/quais-sao-os-precos-das-energias-e-servicos-galp (accessed Jul. 09, 2022).
[25] https://goldenergy.pt/precos-de-referencia/ (accessed Jul. 09, 2022).
[26] https://www.erse.pt/atividade/regulacao/tarifas-e-precos-eletricidade/ (accessed Jul. 09, 2022).

APPENDIX – MATLAB CODE

```
%\-<>---<>---<>---<>---<>---<>---<>---<>---<>---<>---<>---<>-/
%-\---------------CARNOT BATTERY SIMULATION-----------------/-
%--\------Transient Energy Balance Model Applied To--------/--
%---\----Heat Pump/Organic Rankine Cycles Coupled With----/---
%----\--------------Sensible Heat Storage----------------/----
%-----\\\\\\\\\\\\\\\\\\\\\\\\\\\\\\\\\\\\\\\\\\\\\\\\\\\\\\-----
%------\---Pedro Amado------------------DEM-FCTUC-----/------


%Clear previous log - delete if necessary
clc
clear all

%INITIAL INPUT VARIABLES

%----BOUNDARY CONDITIONS----
%CHARGE MODE (1=charge, -1=discharge, 0=idle)
    charge=-1;

%Storage Fluid Initial Temperature [C]
    Tinit=89.2798

%Env. Temperature [K]
    Tenv_C=25

%Study Duration [h]
    studyperiod=24

%TIME STEP [s]
    deltat=30;

%Electric Energy Cost [€/kWh]
    el_cost_charge=0.0
    el_cost_discharge=0.0

%Previously Obtained Total Costs (if applicable) [€]
    el_cost_totalch=0
    el_cost_totaldch=0
    el_cost_balance=0

%----STOPPING CRITERIA | CHARGE----

%Max. Charge (% of Temperature Range)
stopcriterion_charge=0 %Criterion On/Off
maxcharge=95

%Max. Loss/Charge Ratio (Ploss/Pch)
stopcriterion_loss=0 %Criterion On/Off
maxlossratio=0.5

%Max. Temperature
stopcriterion_Tmax=1
Tmax=90
```

```
%----STOPPING CRITERIA | DISCHARGE----

%T<Tevap_RC - stop if water temperature < RC Evap. temperature
stopcriterion_tevaprc=1 %Criterion On/Off

%Min. Temperature
stopcriterion_Tmin=1
Tmin=70

%----SYSTEM CHARACTERISTICS----

%Storage Volume [m^3]
Vol_storage=5

%Cylinder Length/Diameter ratio
cylratio=2

%Design Temperature Difference for Heat Exchangers (Between Cond./Evap. and water)
    spread_hex=5
    spread_hex_bottom=spread_hex
    %Record Nominal Value
    spread_hex_init=spread_hex
    spread_hex_bottom_init=spread_hex_bottom

%Temperatures
%HP Cold Source Temperature
Thotwater_C=70
Thotwater=Thotwater_C+273.15
    %HP
    Tlow_hp=Thotwater_C-spread_hex_bottom
    Thigh_hp=Tmax+spread_hex
    %RC
    Tlow_rc=Tenv_C+spread_hex_bottom
    Thigh_rc=Tmax-spread_hex
%Working fluids
    %HP
    workfluidhp='r1233zd'
    workfluidrc='r1233zd'

%Machine Isentropic Efficiencies
    %HP
    etascomphp=0.7 %VCHP Compressor
    %RC
    etasexprc=0.7 %RC Expander
    etaspumprc=0.8 %RC Pump

%Avg. Electrical Efficiencies (motor and generator)
eta_el=0.95

%Reference Values for Electrical Power
Powercomp_hp=1000 % HP Compressor Power [W]
Powerexp_rc=1000 % ORC Expander Power [W]
```

```
    %Save original values
    Powercomp_hp_init=Powercomp_hp
    Powerexp_rc_init=Powerexp_rc

%Superheating/Subcooling
    %HP
    superheatinghp=0 % Amount of superheating (after evaporator) in Kelvin
    subcoolinghp=0 %Amount of subcooling (after condenser) in Kelvin
    %RC
    superheatingrc=0 % Amount of superheating (after evaporator) in Kelvin
    subcoolingrc=0 %Amount of subcooling (after condenser) in Kelvin

if round((studyperiod*3600)/deltat,0)~=(studyperiod*3600)/deltat
    disp("Error - time interval inadequate for study period")
    return
end
%----------------HP/ORC PRELIMINARY VALUES-----------------

%--------Simple VCHP with Non-Isentropic Machines--------
%Evaporator and Condenser Temperatures (Celsius)
Tevap_C_HP=Tlow_hp
Tcond_C_HP=Thigh_hp
%Absolute Temperatures
Tevap_HP=Tevap_C_HP+273.15
Tcond_HP=Tcond_C_HP+273.15

%Corresponding Evaporation and Condensation Pressures
Pevap_HP=refpropm('P','T',Tevap_HP,'Q',0.5,workfluidhp)
Pcond_HP=refpropm('P','T',Tcond_HP,'Q',0.5,workfluidhp)

%Pressures of various points
p1_hp=Pevap_HP %Compressor inlet
p2_hp=Pcond_HP %Compressor outlet
p3_hp=Pcond_HP %Expander inlet
p4_hp=Pevap_HP %Expander outlet

%Point 1
tsat1_hp=refpropm('T','P',p1_hp,'Q',1,workfluidhp)
if superheatinghp<0
    superheatinghp=0
end
if superheatinghp==0 % Calculation of properties according to saturation state
    t1_hp=tsat1_hp
    h1_hp=refpropm('H','P',p1_hp,'Q',1,workfluidhp)
    s1_hp=refpropm('S','P',p1_hp,'Q',1,workfluidhp)
else
    t1_hp=tsat1_hp+superheatinghp
    h1_hp=refpropm('H','T',t1_hp,'P',p1_hp,workfluidhp)
    s1_hp=refpropm('S','T',t1_hp,'P',p1_hp,workfluidhp)
end

%Point 2
s2s_hp=s1_hp
```

```
h2s_hp=refpropm('H','P',p2_hp,'S',s2s_hp,workfluidhp)
h2_hp=((h2s_hp-h1_hp)/etascomphp)+h1_hp
t2_hp=refpropm('T','P',p2_hp,'H',h2_hp,workfluidhp)

%Point 3
tsat3_hp=refpropm('T','P',p3_hp,'Q',0,workfluidhp)
if subcoolinghp<0
    subcoolinghp=0
end
if subcoolinghp==0 % Calculation of properties according to saturation state
    t3_hp=tsat3_hp
    h3_hp=refpropm('H','P',p3_hp,'Q',0,workfluidhp)
    s3_hp=refpropm('S','P',p3_hp,'Q',0,workfluidhp)
else
    t3_hp=tsat3_hp-subcoolinghp
    h3_hp=refpropm('H','T',t3_hp,'P',p3_hp,workfluidhp)
    s3_hp=refpropm('S','T',t3_hp,'P',p3_hp,workfluidhp)
end

%Point 4
h4_hp=h3_hp %Isenthalpic expansion
q4_hp=refpropm('Q','P',p4_hp,'h',h4_hp,workfluidhp)

%Specific compressor work
Wcomphp=h2_hp-h1_hp

%Specific energy absorbed in evaporator
Eevaphp=h1_hp-h4_hp

%Specific energy released in condenser
Econdhp=h2_hp-h3_hp

%Mass Flow and Compressor Power - Reference Value
mflow_hp=Powercomp_hp/Wcomphp

%Condenser Power - Reference Value
Powercond_hp=mflow_hp*Econdhp % [W]

%Evaporator Power
Powerevap_hp=mflow_hp*Eevaphp

%HP COP
COPHP=Econdhp/Wcomphp

%Max. Carnot COP
COPCarnot=Tcond_HP/(Tcond_HP-Tevap_HP)

%COP as fraction of theoretical maximum
COPrelative=COPHP/COPCarnot

%--------Simple ORC with Non-Isentropic Machines--------
%Evaporator and Condenser Temperatures (Celsius)
Tevap_C_RC=Thigh_rc
```

```
Tcond_C_RC=Tlow_rc

%Absolute Temperatures
Tevap_RC=Tevap_C_RC+273.15
Tcond_RC=Tcond_C_RC+273.15

%Corresponding Evaporation and Condensation Pressures
Pevap_RC=refpropm('P','T',Tevap_RC,'Q',0.5,workfluidrc)
Pcond_RC=refpropm('P','T',Tcond_RC,'Q',0.5,workfluidrc)

%Pressures of the various points
p1_rc=Pevap_RC %expander inlet
p2_rc=Pcond_RC %expander outlet
p3_rc=Pcond_RC %pump inlet
p4_rc=Pevap_RC %pump outlet

%Point 1
tsat1_rc=refpropm('T','P',p1_rc,'Q',1,workfluidrc) %Saturation Temperature at p1_rc
if superheatingrc<0
    superheatingrc=0
end
if superheatingrc==0
    t1_rc=tsat1_rc
    h1_rc=refpropm('H','P',p1_rc,'Q',1,workfluidrc)
    s1_rc=refpropm('S','P',p1_rc,'Q',1,workfluidrc)
else
    t1_rc=tsat1_rc+superheatingrc
    h1_rc=refpropm('H','T',t1_rc,'P',p1_rc,workfluidrc)
    s1_rc=refpropm('S','T',t1_rc,'P',p1_rc,workfluidrc)
end

%Point 2
s2s_rc=s1_rc
h2s_rc=refpropm('H','P',p2_rc,'S',s2s_rc,workfluidrc) %Isentropic Enthalpy
h2_rc=h2s_rc*etasexprc+h1_rc-(etasexprc*h1_rc) %Real Enthalpy
t2_rc=refpropm('T','P',p2_rc,'H',h2_rc,workfluidrc) %Real Temperature
q2_rc=refpropm('Q','P',p2_rc,'H',h2_rc,workfluidrc) %Real Quality
if q2_rc<1
    disp("2-phase mix after expansion - increase superheating or change fluid")
    return
end

%Point 3
tsat3_rc=refpropm('T','P',p3_rc,'Q',0,workfluidrc)
if subcoolingrc<0
    subcoolingrc=0
end
if subcoolingrc>0
    t3_rc=tsat3_rc-subcoolingrc
    h3_rc=refpropm('H','T',t3_rc,'P',p3_rc,workfluidrc)
    s3_rc=refpropm('S','T',t3_rc,'P',p3_rc,workfluidrc)
else
    t3_rc=tsat3_rc
```

```
    h3_rc=refpropm('H','P',p3_rc,'Q',0,workfluidrc)
    s3_rc=refpropm('S','P',p3_rc,'Q',0,workfluidrc)
end

%Point 4
s4s_rc=s3_rc
h4s_rc=refpropm('H','P',p4_rc,'S',s4s_rc,workfluidrc) %Isentropic Enthalpy
h4_rc=((h4s_rc-h3_rc)/etaspumprc)+h3_rc
t4_rc=refpropm('T','P',p4_rc,'H',h4_rc,workfluidrc)

%Specific Expansion work
Wexprc=h1_rc-h2_rc

%Specific Compression work
Wpumprc=h4_rc-h3_rc

%Specific energy absorbed in evaporator
Eevaprc=h1_rc-h4_rc

%Specific energy released in condenser
Econdrc=h2_rc-h3_rc

%Mass Flow and Expander Power - Reference Value
mflow_rc=Powerexp_rc/Wexprc

%Evaporator Power - Reference Value
Powerevap_rc=mflow_rc*Eevaprc % [W]

%Condenser Power
Powercond_rc=mflow_rc*Econdrc

%Rankine Efficiency
etaRankine=(Wexprc-Wpumprc)/Eevaprc

%Max. Carnot Efficiency
etaCarnot=1-(Tcond_RC/Tevap_RC)

%Efficiency as fraction of theoretical maximum
eta_relative=etaRankine/etaCarnot

%Global Efficiency
etaglobal=etaRankine*COPHP
etaglobal1=(Wexprc-Wpumprc)/Wcomphp

%Carnot Global Efficiency
etaglobalCarnot=etaCarnot*COPCarnot

%Carnot Battery Simulation - fixed coeffs. method
    %Env. Temperature [K]
    Tenv=Tenv_C+273.15

%Loss Heat Transfer Coeff. [W/(m^2.K)]
    %Conductive Resistance - Steel
```

```
    ksteel=50 %[W/(m.K)]
    tsteel=0.01 %[m]
    Rsteel=tsteel/ksteel

    %Conductive Resistance - Insulation
    kins=0.05 %[W/(m.K)]
    tins=0.05 %[m]
    Rins=tins/kins

    %Total Resistance of Solid Materials
    Rsolid=Rsteel+Rins

    %Convective Thermal Resistance
    h=10 %[W/(m.K)]
    Rh=1/h

    %Total Thermal Resistance of Water Tank
    Rtotal=Rsolid+Rh

    %Global Loss Heat Transfer Coeff.
    Uloss=1/Rtotal

%Tank Surface Area [m^2]
    %Inner Dimensions of Cylindrical Storage Tank [m]
    di_storage=((4*Vol_storage)/(cylratio*pi()))^(1/3)
    Li_storage=cylratio*di_storage

    %Outer Diameter of Cylindrical Storage Tank [m]
    do_storage=di_storage+(2*(tsteel+tins))
    Lo_storage=Li_storage+(2*(tsteel+tins))
    Ao_storage=pi()*do_storage*Lo_storage+(2*pi()*((do_storage/2)^2)) %Outer↙
Surface Area

%HEAT EXCHANGER DESIGN - HP CONDENSER
    %Exchanger Heat Transfer Coeff. [W/(m^2.K)]
    U_hp_cond=1000
    %Exchanger Area [m^2]
    A_hp_cond=Powercond_hp/(U_hp_cond*(spread_hex))

%HEAT EXCHANGER DESIGN - RC EVAPORATOR
    %Exchanger Heat Transfer Coeff. [W/(m^2.K)]
    U_rc_evap=1000
    %Exchanger Area [m^2]
    A_rc_evap=Powerevap_rc/(U_rc_evap*(spread_hex))

%HEAT EXCHANGER DESIGN - HP EVAPORATOR
    %Exchanger Heat Transfer Coeff. [W/(m^2.K)]
    U_hp_evap=1000
    %Exchanger Area [m^2]
    A_hp_evap=Powerevap_hp/(U_hp_evap*(spread_hex_bottom))

%HEAT EXCHANGER DESIGN - ORC CONDENSER
    %Exchanger Heat Transfer Coeff. [W/(m^2.K)]
```

```
    U_rc_cond=1000
    %Exchanger Area [m^2]
    A_rc_cond=Powercond_rc/(U_rc_cond*(spread_hex_bottom))

%Storage Fluid
storagefluid='water'

T_C=Tinit
    %Initial Temperature [K]
    T=T_C+273.15

%Pressure [kPa]
pressure=101.325

%Density [kg/m^3]
density=refpropm('D','T',25+273.15,'P',pressure,storagefluid)

%Storage Mass [kg]
m_storage=density*Vol_storage

%Charge and Discharge Power [W]
Pch=0
Pdch=0

%Initial Energy Content
cp=refpropm('C','T',T,'P',pressure,storagefluid)
E=m_storage*cp*T
E_init=E

%------------BEGIN ITERATIVE CYCLE------------
%Initialize first iteration
i=1

for t=0:deltat:(3600*studyperiod)
    if t==0
        %(do nothing)
    else
    if charge==1

    error_bottom=1;
    while abs(error_bottom)>0.01 %Check for power convergence (HP Evaporator)
    error=1;
    while abs(error)>0.01 %Check for power convergence (HP Condenser)

    %--------Simple VCHP with Non-Isentropic Machines--------
    %Absolute Temperatures
    Tevap_HP=Thotwater-spread_hex_bottom;
    Tcond_HP=T+spread_hex;

    %Corresponding Evaporation and Condensation Pressures
    Pevap_HP=refpropm('P','T',Tevap_HP,'Q',0.5,workfluidhp);
    Pcond_HP=refpropm('P','T',Tcond_HP,'Q',0.5,workfluidhp);
```

```
%Pressures of various points
p1_hp=Pevap_HP; %Compressor inlet
p2_hp=Pcond_HP; %Compressor outlet
p3_hp=Pcond_HP; %Expander inlet
p4_hp=Pevap_HP; %Expander outlet

%Point 1
tsat1_hp=refpropm('T','P',p1_hp,'Q',1,workfluidhp);
if superheatinghp<0
    superheatinghp=0;
end
if superheatinghp==0 % Calculation of properties according to saturation state
    t1_hp=tsat1_hp;
    h1_hp=refpropm('H','P',p1_hp,'Q',1,workfluidhp);
    s1_hp=refpropm('S','P',p1_hp,'Q',1,workfluidhp);
    d1_hp=refpropm('D','P',p1_hp,'Q',1,workfluidhp);
else
    t1_hp=tsat1_hp+superheatinghp;
    h1_hp=refpropm('H','T',t1_hp,'P',p1_hp,workfluidhp);
    s1_hp=refpropm('S','T',t1_hp,'P',p1_hp,workfluidhp);
    d1_hp=refpropm('D','T',t1_hp,'P',p1_hp,workfluidhp);
end

%Point 2
s2s_hp=s1_hp;
h2s_hp=refpropm('H','P',p2_hp,'S',s2s_hp,workfluidhp);
h2_hp=((h2s_hp-h1_hp)/etascomphp)+h1_hp;
t2_hp=refpropm('T','P',p2_hp,'H',h2_hp,workfluidhp);

%Point 3
tsat3_hp=refpropm('T','P',p3_hp,'Q',0,workfluidhp);
if subcoolinghp<0
    subcoolinghp=0;
end
if subcoolinghp==0 % Calculation of properties according to saturation state
    t3_hp=tsat3_hp;
    h3_hp=refpropm('H','P',p3_hp,'Q',0,workfluidhp);
    s3_hp=refpropm('S','P',p3_hp,'Q',0,workfluidhp);
else
    t3_hp=tsat3_hp-subcoolinghp;
    h3_hp=refpropm('H','T',t3_hp,'P',p3_hp,workfluidhp);
    s3_hp=refpropm('S','T',t3_hp,'P',p3_hp,workfluidhp);
end

%Point 4
h4_hp=h3_hp; %Isenthalpic expansion
q4_hp=refpropm('Q','P',p4_hp,'h',h4_hp,workfluidhp);

%Specific compressor work
Wcomphp=h2_hp-h1_hp;

%Specific energy absorbed in evaporator
Eevaphp=h1_hp-h4_hp;
```

```
    %Specific energy released in condenser
    Econdhp=h2_hp-h3_hp;

    %Charge Power
    Pch=(Tcond_HP-T)*U_hp_cond*A_hp_cond;

    %Condenser Power
    Powercond_hp=mflow_hp*Econdhp;

    %Update delta-T (match heat transfer to mass flow*delta-h)
    Tcond_HP=T+(Powercond_hp/(A_hp_cond*U_hp_cond));

    error = Pch-Powercond_hp;
    spread_hex = Tcond_HP-T;
    end

%Evaporator Power
Powerevap_hp=mflow_hp*Eevaphp;
%Evaporator heat exchange equation power
Powerevap_hp_hex=(Thotwater-Tevap_HP)*U_hp_evap*A_hp_evap;

%Update delta-T (match heat transfer to mass flow*delta-h)
Tevap_HP=Thotwater-(Powerevap_hp/(A_hp_evap*U_hp_evap));

error_bottom=Powerevap_hp_hex-Powerevap_hp;
spread_hex_bottom=Thotwater-Tevap_HP;
end

%Compressor Power
Powercomp_hp=mflow_hp*Wcomphp; % [W]

%Electrical Work
el_charge=Powercomp_hp*deltat/eta_el;

%Evaporator Energy Consumption in time interval
Eevapcons_hp=Powerevap_hp*deltat;

%Condenser Energy Release in time interval
Econdrelease_hp=Powercond_hp*deltat;

%HP COP
COPHP=Econdhp/Wcomphp;

%Volume Flow at Compressor Inlet
vflow_compin=mflow_hp/d1_hp; %[m^3/s]

end
if charge==-1

error_bottom=1;
while abs(error_bottom)>0.01 %Check for power convergence (ORC Condenser)
error=1;
```

```
while abs(error)>0.01 %Check for power convergence (ORC Evaporator)

%--------Simple ORC with Non-Isentropic Machines--------

%Absolute Temperatures
Tcond_RC=Tenv+spread_hex_bottom;
Tevap_RC=T-spread_hex;

%Corresponding Evaporation and Condensation Pressures
Pevap_RC=refpropm('P','T',Tevap_RC,'Q',0.5,workfluidrc);
Pcond_RC=refpropm('P','T',Tcond_RC,'Q',0.5,workfluidrc);

%Pressures of the various points
p1_rc=Pevap_RC; %expander inlet
p2_rc=Pcond_RC; %expander outlet
p3_rc=Pcond_RC; %pump inlet
p4_rc=Pevap_RC; %pump outlet

%Point 1
tsat1_rc=refpropm('T','P',p1_rc,'Q',1,workfluidrc); %Saturation Temperature at↙
p1_rc
if superheatingrc<0
    superheatingrc=0;
end
if superheatingrc==0
    t1_rc=tsat1_rc;
    h1_rc=refpropm('H','P',p1_rc,'Q',1,workfluidrc);
    s1_rc=refpropm('S','P',p1_rc,'Q',1,workfluidrc);
    d1_rc=refpropm('D','P',p1_rc,'Q',1,workfluidrc);
else
    t1_rc=tsat1_rc+superheatingrc;
    h1_rc=refpropm('H','T',t1_rc,'P',p1_rc,workfluidrc);
    s1_rc=refpropm('S','T',t1_rc,'P',p1_rc,workfluidrc);
    d1_rc=refpropm('D','T',t1_rc,'P',p1_rc,workfluidrc);
end

%Point 2
s2s_rc=s1_rc;
h2s_rc=refpropm('H','P',p2_rc,'S',s2s_rc,workfluidrc); %Isentropic Enthalpy
h2_rc=h2s_rc*etasexprc+h1_rc-(etasexprc*h1_rc); %Real Enthalpy
t2_rc=refpropm('T','P',p2_rc,'H',h2_rc,workfluidrc); %Real Temperature
q2_rc=refpropm('Q','P',p2_rc,'H',h2_rc,workfluidrc); %Real Quality
if q2_rc<1
    disp("2-phase mix after expansion - increase superheating or change fluid")
    return
end

%Point 3
tsat3_rc=refpropm('T','P',p3_rc,'Q',0,workfluidrc);
if subcoolingrc<0
    subcoolingrc=0;
end
if subcoolingrc>0
```

```
    t3_rc=tsat3_rc-subcoolingrc;
    h3_rc=refpropm('H','T',t3_rc,'P',p3_rc,workfluidrc);
    s3_rc=refpropm('S','T',t3_rc,'P',p3_rc,workfluidrc);
else
    t3_rc=tsat3_rc;
    h3_rc=refpropm('H','P',p3_rc,'Q',0,workfluidrc);
    s3_rc=refpropm('S','P',p3_rc,'Q',0,workfluidrc);
end

%Point 4
s4s_rc=s3_rc;
h4s_rc=refpropm('H','P',p4_rc,'S',s4s_rc,workfluidrc); %Isentropic Enthalpy
h4_rc=((h4s_rc-h3_rc)/etaspumprc)+h3_rc;
t4_rc=refpropm('T','P',p4_rc,'H',h4_rc,workfluidrc);

%Specific Expansion work
Wexprc=h1_rc-h2_rc;

%Specific Compression work
Wpumprc=h4_rc-h3_rc;

%Specific energy absorbed in evaporator
Eevaprc=h1_rc-h4_rc;

%Specific energy released in condenser
Econdrc=h2_rc-h3_rc;

%Discharge Power [W]
Pdch=(T-Tevap_RC)*U_rc_evap*A_rc_evap;

%Evaporator Power
Powerevap_rc=mflow_rc*Eevaprc; % [W]

%Update delta-T (match heat transfer to mass flow*delta-h)
Tevap_RC=T-(Powerevap_rc/(A_rc_evap*U_rc_evap));

error = Pdch-Powerevap_rc;
spread_hex = T-Tevap_RC;
end

%Condenser Power
Powercond_rc=Econdrc*mflow_rc;
%Condenser Power - Heat Exchange Equation
Powercond_rc_hex=(Tcond_RC-Tenv)*A_rc_cond*U_rc_cond;

%Update delta-T (match heat transfer to mass flow*delta-h)
Tcond_RC=Tenv+(Powercond_rc/(A_rc_cond*U_rc_cond));

error_bottom = Powercond_rc_hex-Powercond_rc;
spread_hex_bottom = Tcond_RC-Tenv;
end

%Expander Power
```

```
Powerexp_rc=mflow_rc*Wexprc; %[W]

%Pump Power
Powerpump_rc=mflow_rc*Wpumprc; %[W]

%Electrical Work
el_discharge=(Powerexp_rc-Powerpump_rc)*deltat*eta_el;

%Evap. Energy Consumption at each time interval
Eevapcons_rc=Powerevap_rc*deltat;

%Rankine Efficiency
etaRankine=(Wexprc-Wpumprc)/Eevaprc;

%Volume Flow at Expander Inlet
vflow_expin=mflow_rc/d1_rc; %[m^3/s]
end

    %Charge and Discharge Power - Standby
    if charge==0
        Pdch=0;
        Pch=0;
    end

    %Storage heat capacity [J/(kg.K)]
    cp=refpropm('C','T',T,'P',pressure,storagefluid);

    %Loss Power
    Ploss=Uloss*(T-Tenv)*Ao_storage;
    %Ploss=1000000;

    %Loss Energy
    Eloss=Ploss*deltat;

    %Energy Balance
    E=E-(Ploss*deltat)+(Pch*deltat)-(Pdch*deltat);

    %Temperature
    T=E/(m_storage*cp);
    T_C=T-273.15;

    %Log Values
    tlog(i)=t;
    T_Clog(i)=T_C;
    Plosslog(i)=Ploss;
    Elosslog(i)=Eloss;
    Elog(i)=E;
    cplog(i)=cp;
    spreadhexlog(i)=spread_hex;
    spreadhexbottomlog(i)=spread_hex_bottom;
    if charge==1
    Pchlog(i)=Pch;
    elchargelog(i)=el_charge;
```

```
    powercomplog(i)=Powercomp_hp;
    Ecomplog(i)=Powercomp_hp*deltat;
    %Econdhplog(i)=Econdhp;
    COPlog(i)=COPHP;
    Powercondhplog(i)=Powercond_hp;
    temppercentlog(i)=((T-(Tinit+273.15))/(Tcond_HP-(Tinit+273.15)))*100;
    Powerevaphplog(i)=Powerevap_hp;
    Econdreleasehplog(i)=Econdrelease_hp;
    Eevapconshplog(i)=Eevapcons_hp;
    vflowcompinlog(i)=vflow_compin;
    Tevaprclog(i)=Tevap_RC;
    end
    if charge==-1
    Pdchlog(i)=Pdch;
    eldischargelog(i)=el_discharge;
    powerexplog(i)=Powerexp_rc;
    powerpumplog(i)=Powerpump_rc;
    Powerevaprclog(i)=Powerevap_rc;
    Powercondrclog(i)=Powercond_rc;
    etaRankinelog(i)=etaRankine;
    Eevapconsrclog(i)=Eevapcons_rc;
    temppercentlog(i)=((T-Tevap_RC)/((Tinit+273.15)-Tevap_RC))*100;
    vflowexpinlog(i)=vflow_expin;
    Epumplog(i)=Powerpump_rc*deltat;
    Eexplog(i)=Powerexp_rc*deltat;
    Tcondhplog(i)=Tcond_HP;
    end
    if charge==0
    temppercentlog(i)=((T-Tenv)/((Tinit+273.15)-Tenv))*100;
    end

%Stopping Criteria - Charge
if charge==1
if stopcriterion_loss==1
if Ploss/Pch>maxlossratio
    break
end
end
if stopcriterion_charge==1
        if temppercentlog(t)>maxcharge
            break
end
end
if stopcriterion_Tmax==1
    if T>(Tmax+273.15)
        break
    end
end
end
%Stopping Criteria - Discharge
if charge==-1
    if stopcriterion_tevaprc==1
        if T<Tevap_RC
```

```
            break
        end
    end
    if stopcriterion_Tmin==1
    if T<(Tmin+273.15)
        break
    end
end
end

%Update iteration index
i=i+1;
    end
end
%Index correction
i=i-1
%------------END OF ITERATIVE CYCLE------------

%Find time constant (36.8% for discharge, 63.2% for charge)
skiptimeconstant=1
if skiptimeconstant==1
timeconstant_t=1
timeconstant=1
else
if charge==1
timeconstant_t=find(round(temppercentlog,1)==90)
end
if charge==-1
timeconstant_t=find(round(temppercentlog,1)==10)
end
if charge==0
timeconstant_t=find(round(temppercentlog,1)==10)
end
timeconstant=round(mean(timeconstant_t),0)
end

%True storage spread [K]
spread=abs(T_Clog(1)-T_Clog(length(T_Clog)));
%Heat Capacity in spread [kWh]
heatcap=abs(Elog(i)-E_init)/(3600*1000);

%Total Loss
Eloss_total=sum(Elosslog)/(3600*1000);


%Total HP Thermal Energy
if charge==1
Econdreleasehp_total=sum(Econdreleasehplog)/(3600*1000);
Eevapconshp_total=sum(Eevapconshplog)/(3600*1000);
Ecomp_total=sum(Ecomplog)/(3600*1000);
else
Econdreleasehp_total=0;
Eevapconshp_total=0;
```

```
Ecomp_total=0;
end

%Total Rankine Thermal Energy
if charge==-1
Eevapconsrc_total=sum(Eevapconsrclog)/(3600*1000);
Epump_total=sum(Epumplog)/(3600*1000);
Eexp_total=sum(Eexplog)/(3600*1000);
else
Eevapconsrc_total=0;
Epump_total=0;
Eexp_total=0;
end

%Total Electrical Values
if charge==1
el_charge_total=sum(elchargelog)/(3600*1000);
el_discharge_total=0;
el_cost_totalch=el_cost_charge*el_charge_total;
end
if charge==-1
el_discharge_total=sum(eldischargelog)/(3600*1000);
el_charge_total=0;
el_cost_totaldch=el_cost_discharge*el_discharge_total;
end
if charge==0
el_discharge_total=0;
el_charge_total=0;
end

%Average Power Values [kW]
%VCHP
if charge==1
power_avg_comp=mean(powercomplog)/1000
power_avg_el=el_charge_total/(t/3600)
power_avg_cond=mean(Powercondhplog)/1000
power_avg_evap=mean(Powerevaphplog)/1000
end
%ORC
if charge==-1
power_avg_pump=mean(powerpumplog)/1000
power_avg_exp=mean(powerexplog)/1000
power_avg_el=el_discharge_total/(t/3600)
end

%Average Pinch Point
spread_hex_avg=mean(spreadhexlog)

%Costs
if charge==1
cost_hp_cond=150*A_hp_cond
cost_hp_evap=150*A_hp_evap
cost_comp=225+(170*max(vflowcompinlog))
```

```
cost_orc_evap=0
cost_orc_cond=0
cost_pump=0
cost_exp=0
end
if charge==-1
cost_orc_evap=150*A_rc_evap
cost_orc_cond=150*A_rc_cond
cost_exp=1.5*(225+(170*max(vflowexpinlog)))
cost_pump=900*(max(powerpumplog)/300)
cost_hp_cond=0
cost_hp_evap=0
cost_comp=0
end
cost_storage=2000+(625*Vol_storage)
cost_electronics=4000

%Display Results
isentropicdebug=["ISENTROPIC EFFICIENCY DEBUG" "VALUES MUST MATCH INITIAL INPUT";"↙
ORC EXPANDER" (h1_rc-h2_rc)/(h1_rc-h2s_rc);"ORC PUMP" (h4s_rc-h3_rc)/(h4_rc-↙
h3_rc);"VCHP COMPRESSOR" (h2s_hp-h1_hp)/(h2_hp-h1_hp)]
results_hex=["HP Condenser Power [W]" Powercond_hp;"HP Condenser U [W/(m^2.K)]"↙
U_hp_cond;"HP Cond. Heat Transfer Area [m^2]" A_hp_cond;"RC Evaporator Power [W]"↙
Powercond_hp;"RC Evaporator U [W/(m^2.K)]" U_rc_evap;"RC Evap. Heat Transfer Area↙
[m^2]" A_rc_evap]
results_storage=["Storage Spread [C]" spread;"Min. Temperature [C]" min(T_Clog);"↙
Max. Temperature [C]" max(T_Clog);"Approx. Energy Contained in Spread [kWh]"↙
heatcap; "alt. calculation" abs(Eloss_total-↙
Econdreleasehp_total+Eevapconsrc_total)]
results_el=["El. Energy in Charge [kWh]" el_charge_total;"El. Energy in Discharge↙
[kWh]" el_discharge_total;"Charging Cost [€]" round(el_cost_totalch,2);"Discharge↙
Value" round(el_cost_totaldch,2);"Net Profit [€]" round((el_cost_totaldch-↙
el_cost_totalch),2);"Current Balance" round((el_cost_totaldch-↙
el_cost_totalch+el_cost_balance),2)]
if charge==1
results_hp=["HP Cond. Energy Release [kWh]" Econdreleasehp_total;"HP COP"↙
Econdreleasehp_total/el_charge_total; "HP COP with loss" heatcap/el_charge_total]
end
if charge==-1
results_orc=["ORC Evaporator Consumption [kWh]" Eevapconsrc_total;"ORC Efficiency"↙
el_discharge_total/Eevapconsrc_total;"ORC Efficiency with loss"↙
el_discharge_total/heatcap]
end
%Stopping Criteria Results - Charge
if charge==1
if stopcriterion_loss==1
if Ploss/Pch>maxlossratio
    criteriadisp_PlossPch=["STOPPING CRITERION -" "Ploss/Pch exceeds" maxlossratio]
end
end

if stopcriterion_charge==1
       if temppercentlog(t)>maxcharge
```

```
            criteriadisp_charge=["STOP CRITERION - " "Storage charged to" maxcharge↙
"%"]
end
end
if stopcriterion_Tmax==1
        if T>(Tmax+273.15)
            criteriadisp_Tmax=["STOPPING CRITERION -" "Max. Temperature of" T_C↙
"reached after" t/3600 "hours"]
        end
end
end

%Stopping Criteria Results - Discharge
if charge==-1
    if stopcriterion_tevaprc==1
        if T<Tevap_RC
            criteriadisp_tevaprc=["STOPPING CRITERION -" "Storage Temperature below↙
ORC Evaporator Temperature"]
        end
    end
    if stopcriterion_Tmin==1
        if T<(Tmin+273.15)
            criteriadisp_Tmin=["STOPPING CRITERION -" "Minimum Temperature of" T_C↙
"reached after" t/3600 "hours"]
        end
    end
end

%Matrices for excel export
if charge==1
excelmat_charge=["Nominal Pinch Point [°C]" "Max. Storage Temperature [°C]" "Min.↙
Storage Temperature [°C]" "Storage Volume [m^3]" "Compressor Ref. Power [kW]"↙
"Energy in Storage Spread [kWh]" "Total Thermal Loss [kWh]" "HP Condenser Area↙
[m^2]" "HP Evaporator Area [m^2]" "Global COP" "Global COP w/loss" "Charge Electric↙
Consumption [kWh]" "Compressor Work [kWh]" "Condenser Energy Release [kWh]"↙
"Evaporator Energy Consumption [kWh]" "Charge Time [h]" "Average Compressor Power↙
[kW]" "Max. Compressor Power [kW]" "Min. Compressor Power [kW]" "Avg. Condenser↙
Pinch Point [K]" "VCHP Mass Flow [kg/s]" "Compressor Cost [€]" "VCHP Condenser Cost↙
[€]" "VCHP Evaporator Cost [€]"; spread_hex_init Tmax Tmin Vol_storage↙
Powercomp_hp_init/1000 heatcap Eloss_total A_hp_cond A_hp_evap↙
Econdreleasehp_total/el_charge_total heatcap/el_charge_total el_charge_total↙
Ecomp_total Econdreleasehp_total Eevapconshp_total t/3600 power_avg_comp max↙
(powercomplog)/1000 min(powercomplog/1000) spread_hex_avg mflow_hp cost_comp↙
cost_hp_cond cost_hp_evap];
end
if charge==-1
excelmat_discharge=["Nominal Pinch Point [°C]" "Max. Storage Temperature [°C]"↙
"Min. Storage Temperature [°C]" "Storage Volume [m^3]" "Expander Ref. Power [kW]"↙
"Energy in Storage Spread [kWh]" "Total Thermal Loss [kWh]" "ORC Evaporator Area↙
[m^2]" "ORC Condenser Area [m^2]" "Global ORC Eff." "Global ORC Eff. w/loss"↙
"Discharge Electric Generation [kWh]" "Expander Work [kWh]" "Pump Work [kWh]"↙
"Evaporator Energy Consumption [kWh]" "Discharge Time [h]" "Average Expander Power↙
[kW]" "Average Pump Power [kW]" "Max. Expander Power [kW]" "Min. Expander Power↙
```

```
[kW]" "Max. Pump Power [kW]" "Avg. Evaporator Pinch Point [K]" "ORC Mass Flow
[kg/s]" "Expander Cost [€]" "Pump Cost [€]" "ORC Evaporator Cost [€]" "ORC
Condenser Cost [€]" "Storage Cost [€]" "Electronics Cost [€]"; spread_hex_init Tmax
Tmin Vol_storage Powerexp_rc_init/1000 heatcap Eloss_total A_rc_evap A_rc_cond
el_discharge_total/Eevapconsrc_total el_discharge_total/heatcap el_discharge_total
Eexp_total Epump_total Eevapconsrc_total t/3600 power_avg_exp power_avg_pump max
(powerexplog)/1000 min(powerexplog)/1000 max(powerpumplog)/1000 spread_hex_avg
mflow_rc cost_exp cost_pump cost_orc_evap cost_orc_cond cost_storage
cost_electronics];
end

return
%Plots
hold on
%Water
plot((tlog/3600),T_Clog)
axis([0 4 70 90])
plot((tlog/3600),Plosslog/1000)
axis([0 4 0 1.5])

%VCHP
plot((tlog/3600),COPlog)
plot((tlog/3600),Powercondhplog/1000)
plot((tlog/3600),powercomplog/1000)
plot((tlog/3600),Powerevaphplog/1000)

%ORC
plot((tlog/3600),etaRankinelog*100)
plot((tlog/3600),Pdchlog/1000)
plot((tlog/3600),Powerevaprclog/1000)
plot((tlog/3600),powerexplog/1000)
plot((tlog/3600),powerpumplog/1000)
plot((tlog/3600),Powercondrclog/1000)

%Other
plot((tlog/3600),vflowexpinlog)
plot((T_Clog),spreadhexlog)
plot((T_Clog),spreadhexbottomlog)
```